THESIS APPROVAL

GRADUATE SCHOOL, KASETSART UNIVERSITY

Master of Engineering (Chemical Engineering)
DEGREE

Chemical Engineering
FIELD

Chemical Engineering
DEPARTMENT

TITLE: Study of Conformation and Drug Release Mechanism of Doxorubicin Conjugated Glycol Chitosan Nanoaggregates by Molecular Modeling

NAME: Ms. Jirapat Boonmee

THIS THESIS HAS BEEN ACCEPTED BY

THESIS ADVISOR
(Associate Professor Thongchai Srinophakun, Ph.D.)

THESIS CO-ADVISOR
(Assistant Professor Manop Charoenchaitrakool, Ph.D.)

DEPARTMENT HEAD
(Associate Professor Phungphai Phanawadee, D.Sc.)

APPROVED BY THE GRADUATE SCHOOL ON _____

DEAN
(Associate Professor Gunjana Theeragool, D.Agr.)

THESIS

STUDY OF CONFORMATION AND DRUG RELEASE MECHANISM OF DOXORUBICIN CONJUGATED GLYCOL CHITOSAN NANOAGGREGATES BY MOLECULAR MODELING

JIRAPAT BOONMEE

A Thesis Submitted in Partial Fulfillment of
the Requirements for the Degree of
Master of Engineering (Chemical Engineering)
Graduate School, Kasetsart University
2009

Jirapat Boonmee 2009: Study of Conformation and Drug Release Mechanism of Doxorubicin Conjugated Glycol Chitosan Nanoaggregates by Molecular Modeling. Master of Engineering (Chemical Engineering), Major Field: Chemical Engineering, Department of Chemical Engineering. Thesis Advisor: Associate Professor Thongchai Srinophakun, Ph.D. 83 pages.

This research studied the geometry parameters of a drug delivery system which consisted of anti-cancer drug, doxorubicin, conjugated with glycol chitosan polymer via *cis*-aconityl linkage. Molecular energy of this drug carrier showed that the *cis*-aconityl linkage can improve the molecular structure in order to control burst drug release under blood pressure. Doxorubicin release mechanism from the linkage was also studied. The *cis*-aconityl had pH-sensitive behavior. The activated energies of doxorubicin release mechanism in acid determined by B3LYP/6-31G//PM3 method were 122.41, 119.27, 160.18 and 222.22 kcal/mole and by B3LYP/6-31G//HF/6-31G method were 54.23, 109.28, 219.98 and 980.49 kcal/mole with mono-, di-, tri-, and quanta-ethylene glycol, respectively. The activated energies of this mechanism in normal condition by B3LYP/6-31G//PM3 method were 379.06, 342.03 and 433.17 kcal/mole and by B3LYP/6-31G//HF/6-31G method were 387.94, 325.67 and 444.78 kcal/mole with mono-, di- and tri(ethylene glycol), respectively. Interpreting from these energies, the doxorubicin can be released in acid solution, but not in normal solution because of too high activated energy. The length of ethylene glycol chains in glycol chitosan polymer has an effect on drug carrier conformation and drug release. As the length of ethylene glycol increases, the structure of the carrier is more stable and reduces the released mechanism of doxorubicin. Glycol chitosan polymer can also be degraded in acid solution.

_____ _____ __ / __ / ____

Student's signature Thesis Advisor's signature

ACKNOWLEDGEMENT

I am indebted to many people who directly or indirectly helped me in performing this research and preparing this report. I would like to express my appreciation to my thesis advisor, Assoc. Prof. Dr. Thongchai Srinophakun for his valuable suggestions and recommendations during the thesis period as well as for his revisions in my report. Respective thanks go to my major committees, Assoc. Prof. Dr. Phungphai Phanawadee, Asst. Prof. Dr. Manop Charoenchaitrakool and graduate school representative, Dr. Patcharin Worathanakul for their great comments and suggestions.

I would like to sincerely thank to all CPCO memberships of Department of Chemical Engineering, Kasetsart University, especially; Mr. Pirawat Thongjun and Ms. Suwalee Martkumchan, for their incredible helps, supports and suggest me in molecular modeling program. This thesis was supported by National Center of Excellence for Petroleum, Petrochemicals and Advanced Materials, S&T Postgraduate Education and Research Development Office (PERDO) and Asian Development Bank (ADB).

Finally, heartful thank to my family and friends for standing beside me all times even sorrow. I would like to dedicate this thesis to my mother who always gives gentle love and special care to me.

Jirapat Boonmee

April 2009

TABLE OF CONTENTS

Page

LIST OF TABLES

LIST OF TABLES (Continued)

LIST OF TABLES (Continued)

LIST OF FIGURES

LIST OF FIGURES (Continued)

LIST OF FIGURES (Continued)

LIST OF ABBREVIATIONS

6-31G	=	Basis set: (1s: 6 GTO's; 2s (2px etc.): 3 GTO's; 2s'(2px' etc.): one GTO)
B3LYP	=	Becke 3-term functional; Lee, Yang, Parr exchange
B3LYP/6-31G//HF/6-31G	=	Molecular energy calculation form optimized by HF/6-31G
B3LYP/6-31G//PM3	=	Molecular energy calculation form optimized by PM3
DOX	=	Doxorubicin
GAUSSIAN 03W	=	GAUSSIAN software for Windows
GaussViewW	=	GaussView software for window
GC	=	Glycol-chitosan
GC/DOX	=	Doxorubicin is carried on glycol chitosan by H-bonding (carrier based system)
GC-DOX	=	Doxorubicin conjugated glycol chitosan by *cis*-aconityl linkage
HF/6-31G basis	=	Optimization by Hartree-Fock method with set 6-31G
H_2O	=	Water
H_3O^+	=	Hydronium ion
PEG	=	Polyethylene glycol
PM3	=	MNDO parameter method number 3
Ψ	=	Wave function

STUDY OF CONFORMATION AND DRUG RELEASE MECHANISM OF DOXORUBICIN CONJUGATED GLYCOL CHITOSAN NANOAGGREGATES BY MOLECULAR MODELING

INTRODUCTION

In recent years, people suffer from tumor sick. Chemotherapy is an interesting method to treat these tumors. It can be used with a combination of any of other cancer treatment such as operation, irradiation and hormonetherapy.

Doxorubicin is one of the most useful anti-tumor drug with wide range of activity against malignancy such as breast cancer, lung cancer, haematological malignancies, ovarian cancer, bladder cancer, thyroid cancer, gastric cancer, acute lymphoblastic leukemia, Kaposi's sarcoma related to acquired immunodeficiency syndrome (AIDS), and so on (U.S. National library of medicine, 2007). However, it is not the first selection in the clinic because of its lower sensitivity against tumor cells. To improve the anti-tumor activity and reduce the side effects of doxorubicin, it needs polymeric micelle delivery systems (Hu *et al*., 2007).

One strategy of drug delivery system using the polymeric amphiphiles with both hydrophilic and hydrophobic groups form self-assemblies composed of an inner core of hydrophobic segments and an outer shell of hydrophilic segments in aqueous media. The hydrophobic core serves as micro-reservoirs for hydrophobic drugs (Son *et al*., 2003).

Doxorubicin is incorporated into the hydrophobic core of micelle by hydrophobic interaction (Nishiyama *et al*., 2001) and/or electronic interaction (Kabanov *et al*., 1996). These interactions are weak between core-forming blocks and incorporated drugs. Polymer micelles are easily deformable and disassemble because intravenous injections of micellar solution are associated with extreme dilutions by

blood, which result in the leakage of loaded drugs (Ye *et al*., 2008). This is one limitation of polymeric micelles as drug delivery carriers.

A strategy of drug delivery system development is conjugation of anti-tumor drug with polymer chains by chemical linkage. This strategy can improve the interaction between the drug and polymer in order to control drug release rate and reduce the burst release (Kataoka *et al.,* 2001).

Various experimental measurements can provide information necessary for improving controlled drug delivery system. It would be highly beneficial if one could predict the structure, interaction and mechanism by computer simulations. If this possible, the number of inconvenient and sometimes hazardous and/or expensive experiments can be reduced. Consequently, molecular modeling technique is employed to investigate the structure, drug release mechanism and degradation of polymer in solutions effect of a model drug delivery system, the conjugated of doxorubicin and glycol chitosan via *cis*-aconityl linkage. Effect of polyethylene glycol chain length is also studied here.

OBJECTIVES

1. To apply the molecular modeling in order to study and simulate the conformation of doxorubicin conjugated glycol chitosan polymer (GC-DOX) molecule.

2. To propose the doxorubicin release mechanism from this carrier and glycol chitosan polymer biodegradation mechanism in acid and normal conditions.

3. To study the effect of polyethylene glycol chain length to drug carrier formation, drug release mechanism and polymer degradation.

Scopes of work

1. The comparison of molecular energy between doxorubicin conjugated glycol chitosan by *cis*-aconityl linkage (GC-DOX) and without conjugated molecule (GC/DOX) in order to indicate the stability of these drug carriers.

2. The release mechanism from GC-DOX is carried on acid and normal solutions.

3. The biodegradation of glycol chitosan polymer is investigated in acid and normal solutions.

4. GaussViewW and GAUSSIAN 03W version for Windows software are used as simulation software.

Expected results

1. Energetic of interaction between doxorubicin and glycol chitosan via *cis*-aconityl linkage and drug release mechanism can be determined by molecular modeling.

2. The *cis*-aconityl linkage can improve the interaction of doxorubicin delivery system and polyethylene glycol chain can strengthen the structure.

3. The *cis*-aconityl is a pH-sensitive linkage with hydrolysis.

4. The glycol chitosan polymer can easily deform in acid solution.

LITERATURE REVIEWS

In treating the cancer cell, the method is very important because of the side effect on normal cell. This research expects to study drug delivery system to cancer cell which consists of drug and carrier system. The drug carrier structure has several formations such as encapsulation, hydrogel, nanoaggregation and micelle.

Drug delivery

The doxorubicin (DOX), which is a member of the anthracycline ring antibiotics, is used widely in cancer therapy. The medication is used to treat in the human organelles such as breast, ovarian, transitional cell bladder, bronchogenic lung, thyroid, gastric, soft tissue and osteogenic sarcomas, neuroblastoma, and Wilms' tumor. The treatment must be minimized the undesirable side effects. The side effects from doxorubicin are common and include nausea and vomiting, loss appetite, diarrhea, swallowing difficult, thinned or brittle hair, skin irritation, darkening of fingernail or toenails, and swelling (U.S. National library of medicine, 2007). The efficacy of present cancer chemotherapy is mainly limited by the toxicity associated with the anticancer drugs to normal tissues. Therefore, the doxorubicin chemotherapy needs drug delivery system in order to bring it to target cells.

Steinfeld *et al*. (2006) studied doxorubicin to treat the T lymphocytes cancer cell by mobilizing immune cells as therapeutic drug carrier systems. The doxorubicin treatment needs drug carrier to bring to cancer cell target because this molecule has side effect such as heart damage, nausea and vomit. This effect may last up to 24-48 hours after treatment. The carrier molecule can be used in many forms such as encapsulation, nanoaggregation, hydrogel, and micelle formation.

The chitosan sponge delivery is prepared by freeze-drying partially N-acetylated chitosan gels and crosslinked by glytaraldehyde in chitosan solution. From this study, the pH of dissolution media and the drug content of the sponges affected the release of drug. The drug released at pH 1.2 is faster than at pH 7.4. The release of

drug can be controlled by varying the drug content, the acetylation and cross linking. The delayed drug release came from the decreased chitosan solubility by either N-acetylation or crosslinking (Oungbho and Muller, 1997).

The experiments are studied in efficiency to treat at the inoculation of murine macrophage cells into Balb/c mice. Mice are randomized into groups such as untreated controls, empty chitosan nanoparticles, doxorubicin in solution, dextran–doxorubicin conjugate, chitosan nanoparticle entrapped dextran-doxorubicin, and chitosan nanoparticle entrapped dextran-doxorubicin conjugate. In this study, the drug conjugate was attempted to couple the drug with dextran and capsulate in hydrogel nanoparticles. The size of these nanoparticles was 100±10 nm diameter determined by quasi-elastic light scattering. In the results, the conjugation of doxorubicin with dextran effectively reduces toxicity of the free drug and optimizes the drug efficacy by its low molecular weight. Nevertheless, the size of the conjugate is not necessarily large enough to exploit the enhanced permeability and retention (EPR) effect of macromolecular therapeutics (Mitra *et al*., 2001).

The doxorubicin can be used in drug delivery by conjugation with dextran. The mice are injected intravenously with both dextran-doxorubicin conjugates and the encapsulated conjugation in chitosan nanoparticles. This drug conjugation decreases tumor volume after 4 weekly injections. The tumor volume of the mice treated with the encapsulated conjugation is lower than the tumors treated with the conjugate alone. However, the treatment with doxorubicin alone did not decrease the tumor volume, because this molecule can bind both normal and cancer cell. Then, this drug has possibility to bind with other cell (Brannon-Peppas and Blanchette, 2004).

Cheng *et al.* (2006) studied the functionalized poly(D,L-lactide–co–glycolide)–block–poly(ethylene glycol) nanoparticles for *in vivo* targeted drug delivery. The nanoparticle size has been shown to significantly affect the biodistribution of targeted and non-targeted NPs in an organ specific manner. Herein, the nanoparticles have developed from carboxy-terminated poly(D,L-lactide–co–glycolide)–block–poly(ethylene glycol) polymer. The effects of altering the following

formulation parameters on the size of NPs are studied by: 1) polymer concentration, 2) drug loading, 3) water miscibility of solvent, and 4) the ratio of water to solvent. The study found that the volumetric size of treatment correlates linearly with polymer concentration and the nanoparticle size can be controlled together with targeted delivery. These nanoparticles may be used for favorable biodistribution and development of clinically relevant targeted therapies.

Park *et al.* (2006) studied self-assembled nanoparticles, which is formed by polymeric amphiphiles. These nanoparticles of polymeric amphiphiles are demonstrated to accumulate in solid tumors by the enhanced permeability and retention effect. The glycol chitosan can be modified in forming nano-sized self-aggregates by chemical conjugation of doxorubicin to the backbone of glycol chitosan. The self-aggregate biodistribution is evaluated by using tissues obtained the tumor-bearing mice. When self-aggregates loaded with doxorubicin are administered into the tumor-bearing mice via the tail vein, these self-aggregates are lower toxicity than anti-tumor activity to free doxorubicin. The promising potential of self-aggregates on the basis of glycol chitosan can carry the hydrophobic anti-tumor agent.

The chitosan has poor water solubility. Chan *et al*. (2007) synthesizes the chitosan-poly(ethylene glycol) in drug delivery. The poly(ethylene glycol) can increase the chitosan-g-poly(ethylene glycol) solubility. The folate conjugation may improve gene transfection efficiency due to promoted uptake of folate receptor bearing tumor cells. In this study, the poly(ethylene glycol) can form with folate in folate-poly(ethylene glycol)-grafted chitosan structure for targeted plasmid DNA delivery to tumor cells. From this study, the doxorubicin can be carried by chitosan capsule. This capsule can protect and carry drug. Some functional group are needed to detect the cancer cell such as poly(ethylene glycol). The poly(ethylene glycol) is a polyether diol, which is amphiphilic. This amphiphilic molecule can be dissolved in aqueous and organic solvents.

Chemical linkage

Shen and Ryser (1981) reported that the *cis*-aconityl linkage between daunomycin and Affi-Gel 701 (aminoetylpolyacrylamide beads) and to poly (D-lysine). The *cis*-aconityl linkage had pH-sensitive behavior with a hydrolysis half-life of less than 3 h at pH 4 and more than 96 h at pH 6 or higher. Thin layer chromatography and cytotoxic tested in cultured cells indicate that the product of hydrolysis was unaltered daunomycin. These Affi-Gel conjugated presented for 3 days in the culture medium of WEHI-5 cells at neutral pH had little or no growth inhibitory effect. N-*cis*-aconityl daunomycin-poly(D-lysine) conjugates, however, added to WEHI-5 cells under comparable conditions caused a 90% inhibition of cell growth. In contrast, comparable addition of N-maleyl daunomycin-poly(D-lysine) conjugates was not inhibitory. N-*cis*-aconityl daunomycin-poly(D-lysine) entered cells and reached the lysosomal compartment, and that the *cis*-aconityl spacer releaseed daunomycin from poly(D-lysine) in the acidic milieu of lysosomes due to the participation of a free *cis*-carboxylic group. This releasing mechanism should be applicable to other drug-macromolecular conjugates.

Al-Shamkhani and Duncan (1999) synthesized the covalent conjugates of alginate and the antitumor agent daunomycin (DNM). It formed stable in the circulation and allowed release of the drug in the acidic milieu of endosomal and lysosomal compartments of tumor cells or the slightly acidic extracellular fluid of some solid tomors. DNM was first reacted with *cis*-aconitic anhydride to produce N-*cis*-aconityl-DMN and then subsequently bound to the amino-modified alginate using the water-soluble carbodiimide 1-ethyl-3-(3-dimethylaminopropyl) carboiimide (EDC). In vitro release studies showed that DMN was released from the conjugates (approx. 22-60% /48 h) under acidic conditions (pH 5 and 6) with minimal release occurring at neutral pH (approx. 2-4% /48 h).

Two isomers of *cis*-aconytil-daunomycin (cAD) were isolated after the reaction of daunomycin with *cis*-aconitic-anhydride. The structure of the isomers was identified by MS-spectroscopy and ^{1}H and ^{13}C NMR experiments. The two isomers

belong to the *cis*- and *trans*- isomers of the α-monoamide of *cis*-aconityl-daunomycin, respectively. Daunomycin conjugate release depended on pH that different for the two isomers. Comparative analysis of the *in vitro* antitumor effect of the isomers on c26 colon carcinoma and on MDA-MB 435P human breast carcinoma cell lines showed that cAD-1 is more potent than cAD-2, but the extent of differences was tumor cell dependent. The results of this study might be appreciated in the light of the use of acid-labile spacer for the design and preparation of protein/peptide conjugates of drugs by indicating that isomers could posse markedly different biological activity. (Remenyi *et al*., 2003)

The drug carrier usually has some functional group to detect cancer cell target. This cancer cell target is protein molecule. Son *et al*. (2003) studied an *in vivo* tumor targeting test of glycol chitosan nanoaggregates which was carried out with fluorescein isothiocyanate-conjugated glycol chitosan nanoaggregates (FTC-GC) and the doxorubicin conjugated glycol chitosan (GC-DOX) by *cis*-aconityl linkage. To investigate its biodistribution in tumor-bearing rats, the glycol chitosan was labeled with fluorescein isothiocyanate (FITC), which formed nanoaggregates with in aqueous media. The GC-DOX nanoaggregates were acid-sensitive molecule. The GC-DOX could form micelle-like nanoaggregates spontaneously in aqueous media. The doxorubicin molecules were more loaded in GC-DOX nanoaggregates (DOX/GC-DOX) and were injected into the tail vein of tumor-bearing rats. Tumor growth was suppressed over 10 days.

The chitosan is a biodegradable and biocompatible polysaccharide. This chitosan sheet could be used as drug carrier for controlled release. The chitosan sheet is stable in water and degraded with lysozyme or an acidic solution *in vitro*. From the study by Saito *et al.* (2006), the chitosan was a slightly cationic natural polysaccharide which could react with the numerous amino groups. For the drug release, the chitosan was biodegradable and could release drug to target such as urine and liver. The biodegradation of chitosan is mediated by lysozyme. This release depended on specific cells or organs into blood. The enhancement of lysozyme was

probably a biological defensive function, followed by activation of the macrophage system in animals.

From these previous studies, the glycol chitosan carrier and cis-aconityl linkage can release drug in the acidic milieu of the endosomal and lysosomal compartments of tumor cells that contain digestive enzymes (acid hydrolysis) for digest macromolecules or the slightly acidic extracellular fluid of some solid tumors.

Molecular simulations

Frimand and Jalkanen (2002) studied in molecular simulation of propylene oxide by semi-empiracal and *ab initio* methods. This bond length and bond angle from simulation was shown in Table 1. From this study, the *ab initio* method (B3LYP, RHF and MP2) could optimize better than semi-empirical method (AM1, PM3 and SCC-TB). In semi-empirical method, the method SCC-TB could calculate better than PM3 and AM1 methods. In the *ab initio* method, the MP2 could optimize structure of the propylene oxide better than B3LYP and RHF methods, respectively. The 6-31G* and 6-311++G(2d,2p) basis sets gave the bond length and bond angle in optimum structure nearly with experimental data.

Sun *et al*. (2003) used Gaussian 98 to optimize the geometries of common chemical systems. The *ab initio* method was used to simulate. The system included diatomics, N_2, O_2, F_2 and CO, and carbon based organic systems, ethane, ethylene, acetylene, 1,3-butadiene, 1,3,5-hexatriene, benzene, biphenyl, naphtalene graphene, polyethylene and all-trans-polyacetylene. The simulation based on the generalized gradient approximation was very good agreement on bond lengths and angles as compared with experimental value.

Cummins and Gready (2003) used the semi-empirical quantum mechanics method to describe molecular interactions adequately. This simulation studied the enzymatic reaction mechanism, 20 phosphate groups in NADPH cleaved from the ribose ring. In description of intermolecular, the forces in particular had interaction

between atoms. This simulation associated with strong hydrogen bonding. From the study, the semi-empirical AM1 or PM3 method was used to simulate the protein systems. The methods were applied to the calculation of the reaction free energy for the enzymatic reduction of DHF by NADPH cofactor bound to Escherichia coli dihydrofolate reductase. The free energy change for this reduction, calculated using a multiple molecular dynamics simulation, agreement with the experimental results.

Lam *et al.* (2004) studied the hydrophobic molecules effect on the morphology of aqueous solutions of amphiphilic block copolymer, which had potential drug delivery applications. The effect was studied both experimental and simulations. Using cryogenic TEM observations, the micelles could clearly be visualized and their core sizes could be measured. While pure polymer solutions form was spherical micelles with a narrow size distribution, addition of small amounts of hydrophobic drug molecules leaded to distortions in shape, a wider size distribution, and larger average core diameter. Simulations was based on a mesoscale dynamic density functional method with Gaussian chain Hamiltonian and mean-field interactions, as implemented in the MesoDyn code.

Thongjun (2007) studied the released of doxorubicin from glycolchitosan capsule by molecular modeling method. The release mechanism could be studied the polymer breaking of polyglycolchitosan in three conditions; acid, normal and base solution. The doxorubicin could be released in acid and water solutions, but not in base solution because of high activated energy. The amount and length of ethylene glycol chain in glycolchitosan had an effect on drug release. The possibility of micelle formation was studied by B3LYP/6-31G//PM3 method which the ethylene glycol had helps glycolchitosan to form micelle structure.

From the previous molecular simulations studies, the molecular simulation can optimize the molecular structure and predict the possibility of reaction mechanism.

Table 1 The optimised structure of propylene oxide for the six levels of theory MP2, RHF, DFT/B3LYP, AM1, PM3 and SCC-TB together with the experimental structure

	6-31G*							6-311++G(2d,2p)		
	MP2	RHF	B3LYP	SS-TB	AM1	PM3	EXP	MP2	RHF	B3LYP
r(C2-O1)	1.44	1.40	1.43	1.45	1.43	1.43	1.44	1.44	1.40	1.43
r(C3-O1)	1.44	1.40	1.44	1.46	1.44	1.44	1.45	1.45	1.40	1.44
r(C2-C3)	1.47	1.45	1.47	1.49	1.49	1.49	1.08	1.08	1.45	1.47
r(C2-H4)	1.09	1.08	1.09	1.11	1.10	1.10	1.08	1.08	1.07	1.08
r(C2-H5)	1.09	1.08	1.09	1.11	1.10	1.10	1.08	1.08	1.08	1.08
r(C3-H6)	1.09	1.51	1.09	1.51	1.10	1.11	1.50	1.50	1.50	1.50
r(C7-H8)	1.50	1.08	1.09	1.10	1.49	1.50	1.09	1.09	1.08	1.09
r(H7-H9)	1.09	1.09	1.09	1.10	1.12	1.10	1.09	1.09	1.09	1.09
r(C7-H10)	1.09	1.09	1.10	1.10	1.12	1.10	1.09	1.09	1.09	1.09
θ(H4-C2-O1)	115.2	115.2	115.5	114.9	114.5	116.1	112.0	114.7	115.1	115.1
θ(H5-C2-O1)	115.0	115.4	115.3	114.9	114.6	116.4	112.0	114.6	115.1	115.0
θ(H6-C3-O1)	115.2	113.4	113.4	113.7	113.4	114.7	112.0	113.1	113.3	113.0
θ(C7-C3-O1)	113.2	116.5	116.6	116.2	116.1	117.2	115.1	115.9	116.8	116.8
θ(H4-C2-C3)	116.0	120.3	120.2	119.9	120.6	121.5	119.1	119.8	120.1	120.0
θ(H5-C2-C3)	120.1	119.8	119.3	119.9	120.8	121.7	119.1	119.1	119.6	119.2
θ(H6-C3-C2)	119.2	117.4	117.2	118.1	119.5	119.9	119.1	117.1	117.2	119.5
θ(C7-C3-C2)	117.3	122.5	122.4	121.0	121.5	121.1	122.7	121.5	120.6	122.5
θ(H8-C7-C3)	109.9	110.6	110.6	110.9	111.1	112.7	109.5	110.0	110.7	110.7
θ(H8-C7-H9)	108.4	108.2	108.2	108.3	108.3	107.4	109.5	108.5	108.3	108.3
τ(H8-C7-C3-O1)	-43.9	-43.4	-44.2	-40.8	-40.8	-41.7	-43.0	-43.0	-43.4	-43.5

Distances, r, are measured in Å(Angstroms), angles θ and τ in degrees.

Source: Frimand and Jalkanen, (2002)

MATERIALS AND METHODS

This thesis focuses on molecular structure and reaction mechanism simulation. Therefore, computational equipment and software are provided for molecular modeling. High efficiency computers are used to determine geometrical parameters of two drug delivery systems of doxorubicin, doxorubicin in glycol chitosan carrier by H-bonding (GC/DOX) and doxorubicin conjugated glycol chitosan by *cis*-aconityl linkage (GC-DOX). The reaction mechanisms are optimized by transition state method, then calculates the relative energy of each step. The molecular modeling software named GaussViewW and GAUSSIAN 03W will be employed in this work.

Materials

The materials or equipments are shown in the following:

1. High efficiency computers:
   Intel® Xeon™ CPU3.0 GHz 2 processors, 2.0 GB of RAM
   Intel® Pentium® 4 CPU 3.00 GHz processor, 2.0 GB of RAM
   Intel® Core™2 Duo CPU 2.00 GHz processor, 2.0 GB of RAM
   AMD Athlon™ XP 64 bit CPU 2.0 GHz processor, 1 GB of RAM
   AMD Athlon™ XP 64 bit CPU 2.0 GHz processor, 1 GB of RAM
   AMD Athlon™ XP 64 bit CPU 2.0 GHz processor, 1 GB of RAM
   AMD Athlon™ XP 32 bit CPU 2.0 GHz processor, 512 MB of RAM
2. GAUSSIAN 03W and GaussViewW versions for Windows software.

Methods

Molecular modeling is the specific method to determine any molecular structures, which are shown in Figures 1, 2, 3 and 4. The ethylene glycol chains are increased one molecule up to five molecules in both GC/DOX and GC-DOX carriers for studying effect in the formation. This technique can estimate the geometrical parameters in the molecular level such as bond length and charge. These parameters

can be used to calculate the molecular energy. Next step, the molecular energies of GC/DOX molecules (Figure 3) and GC-DOX molecules (Figure 4) are compared.

After the optimization results show the GC-DOX molecular structures are more stable than the GC/DOX, use the optimized GC-DOX molecules to study doxorubicin released mechanism of GC-DOX in two environments, normal and acidic. The final simulation is glycol chitosan polymer degradation mechanism which is studied by bond breaking of di glocosamine(ethylene glycol). The effect of length of ethylene glycol chains to reaction of drug release and degradation of glycol chitosan are also studied. The scheme of this simulation methodology is shown in Figure 5.

In this study, all molecular structures are optimized by semi-empirical PM3 method and *ab initio* HF/6-31G method. Molecular energy of each molecule is calculated by B3LYP/6-31G method which is one of density functional theory (DFT) method. All calculations are performed with the Gaussian 03 program (Foresman and Frisch, 1996).

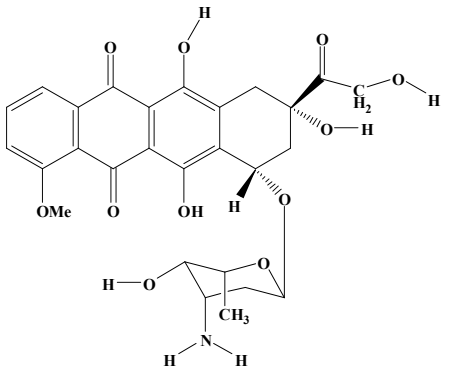

Figure 1 Molecular structure of Doxorubicin

Source: Furgeson *et al*. (2006)

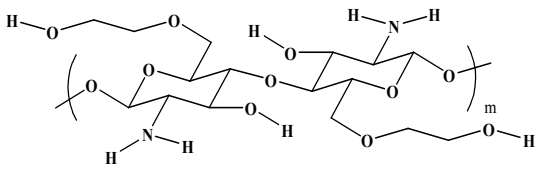

Figure 2 Molecular structure of glucosamine(ethylene glycol) oligomers

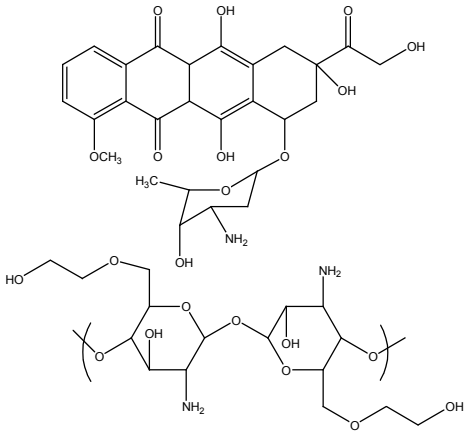

Figure 3 Chemical structure of doxorubicin in glycol chitosan carrier by H-bonding (GC/DOX)

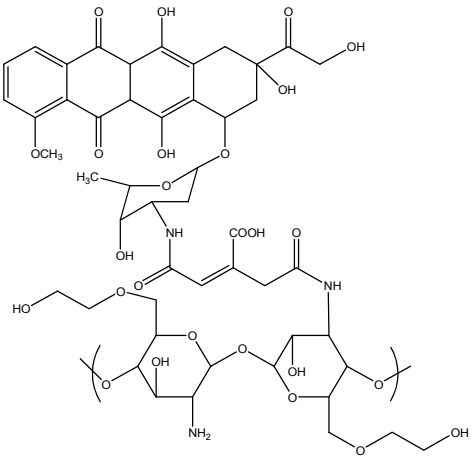

Figure 4 Chemical structure of doxorubicin conjugated glycol chitosan by *cis*-aconityl linkage (GC-DOX)

Source: Son *et al*. (2003)

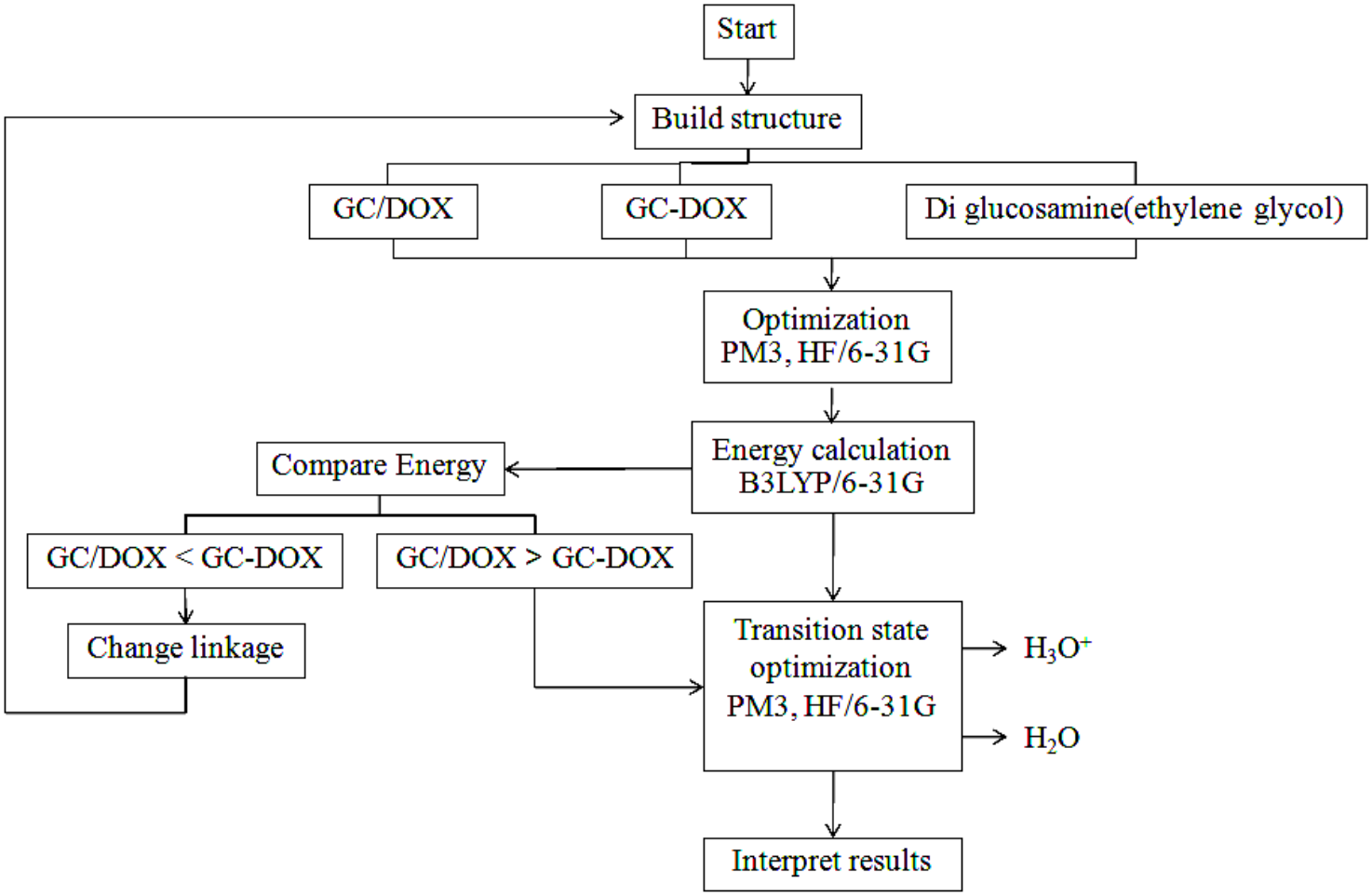

Figure 5 Scheme of drug delivery system simulation in this research

RESULTS AND DISCUSSION

This section proposed the geometrical parameters such as molecular energy, bond length and charge structure in optimization by Gaussian protocol. Drug release mechanism and biodegradation of glycol chitosan polymer in solution effect are also studied. The geometrical parameters of this doxorubicin carrier molecule can be studied by the relationship between optimum structure and optimization step numbers. Molecular energy is calculated to investigate stability of structure. The charge structure of doxorubicin and the glycol chitosan molecules were formulated into the GC/DOX carrier. The length of ethylene glycol chain plays a major role on both doxorubicin and glycol chitosan molecular formation by H-bond and *cis*-aconityl linkage. The doxorubicin release mechanism and the glycol chitosan polymer bond breaking have related the effect of solution environments; normal and acidic.

Geometrical Parameters

The geometrical parameters are firstly considered to propose the optimum conformation of doxorubicin and glycol chitosan via H-bond and *cis*-aconityl linkage. These parameters are molecular energy, charge structure and bond length of molecule. The charge structure is proposed to describe an interaction between doxorubicin and glycol chitosan in GC/DOX molecule. These geometrical parameters are calculated by semi-empirical PM3 and *ab initio* HF/6-31G methods.

Optimum conformation with semi-empirical PM3 and *ab initio* HF/6-31G methods

The optimum structures of doxorubicin and glycol chitosan via H-bond (GC/DOX) and *cis*-aconityl linkage (GC-DOX) are calculated from total molecular energy. The total energy will decrease until reach optimum structure and then obtain the total lowest molecular energy. The total energy decreases along with the molecular optimization steps as shown in Figures 6 and 7.

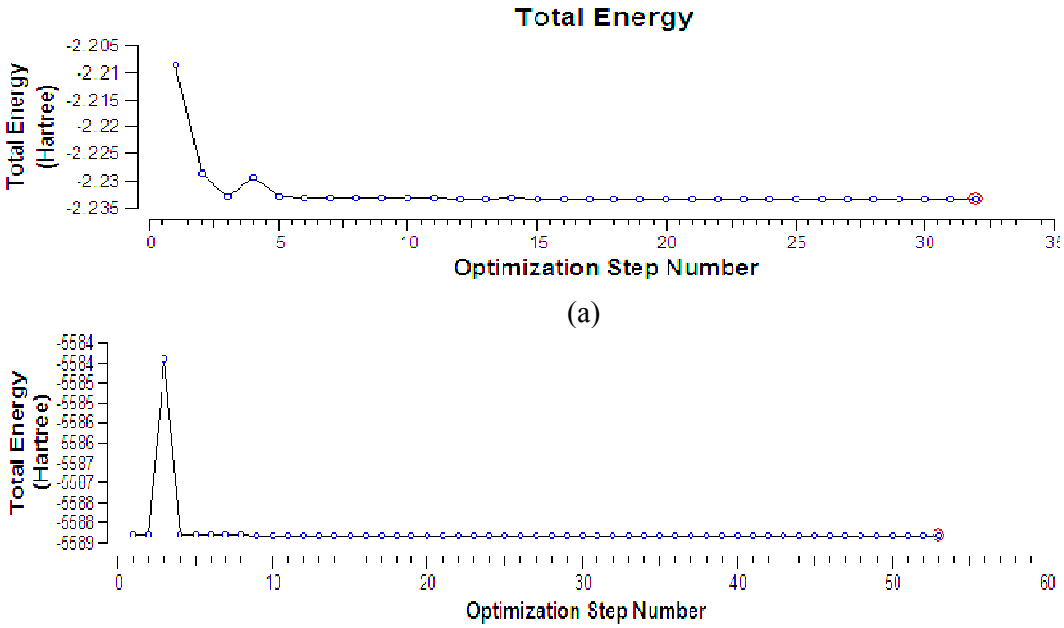

Figure 6 Total energy of GC/DOX with quanta(ethylene glycol) by (a) semi-empirical PM3 and (b) *ab initio* HF/6-31G method

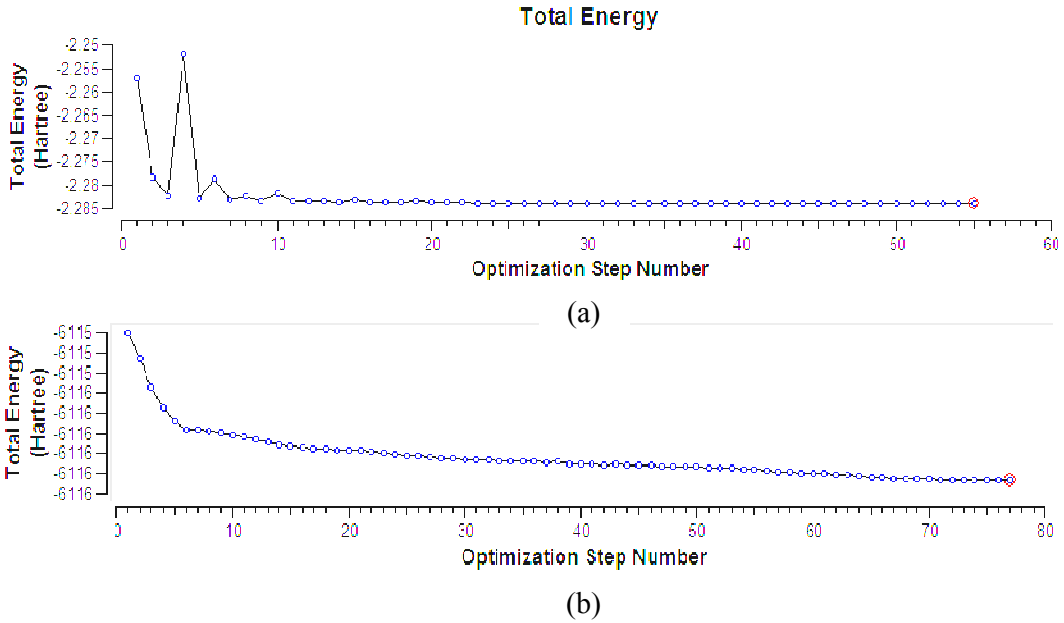

Figure 7 Total energy of GC-DOX with quanta(ethylene glycol) by (a) semi-empirical PM3 and (b) *ab initio* HF/6-31G method

The optimum molecular structures of GC/DOX and GC-DOX molecules are optimized by semi-empirical PM3 and *ab initio* HF/6-31G methods. The GC/DOX with quanta(ethylene glycol) optimization by semi-empirical PM3 method, the optimization is approximately at the step of 32 which stable structure of optimization is in the range of 15-32 steps. The relative energy between input and output from optimization is about -0.025 Hartree (1 Hartree = 627.51 kcal/mol). The stable structure of GC/DOX with quanta(ethylene glycol) which is optimized by *ab initio* HF/6-31G method is in the range of 10-53. For the GC-DOX optimization by semi-empirical PM3 method, the stable structure is in the ranges of 23-55 steps. When *ab initio* HF/6-31G is used to optimization, the stable structure is approximately at the step of 77. The amount of optimization steps by *ab initio* HF/6-31G method has more than the PM3 method. A large amount of optimization steps depend on complexity of that molecule. Sometimes the PM3 method has the optimization step numbers more than the HF method because it depends on initial structure that built up.

The optimum molecular structures of GC/DOX and GC-DOX by semi-empirical PM3 and *ab initio* HF/6-31G methods are shown in Figures 8, 9, 10 and 11, respectively.

The doxorubicin structure has benzene rings which the electron in conjugate double bond can delocalize to next bond in the ring. This electron delocalization makes the doxorubicin structure more stable. From the optimum structures, it can be seen that *ab initio* HF/6-31G method can optimize doxorubicin molecule to the correct planar fused-ring structure and more straight polyethylene glycol chains in GC-DOX molecules, while the semi-empirical PM3 method optimize doxorubicin molecule in non-planar and bent polyethylene glycol chains when the drug carrier has long outer hydrophilic chain. However, the correct structure relates to lower molecular energy in optimization. From the GC/DOX and GC-DOX optimizations, they can be concluded that *ab initio* HF/6-31G method can optimize molecular structures of doxorubicin and polyethylene glycol chain better than semi-empirical PM3 method.

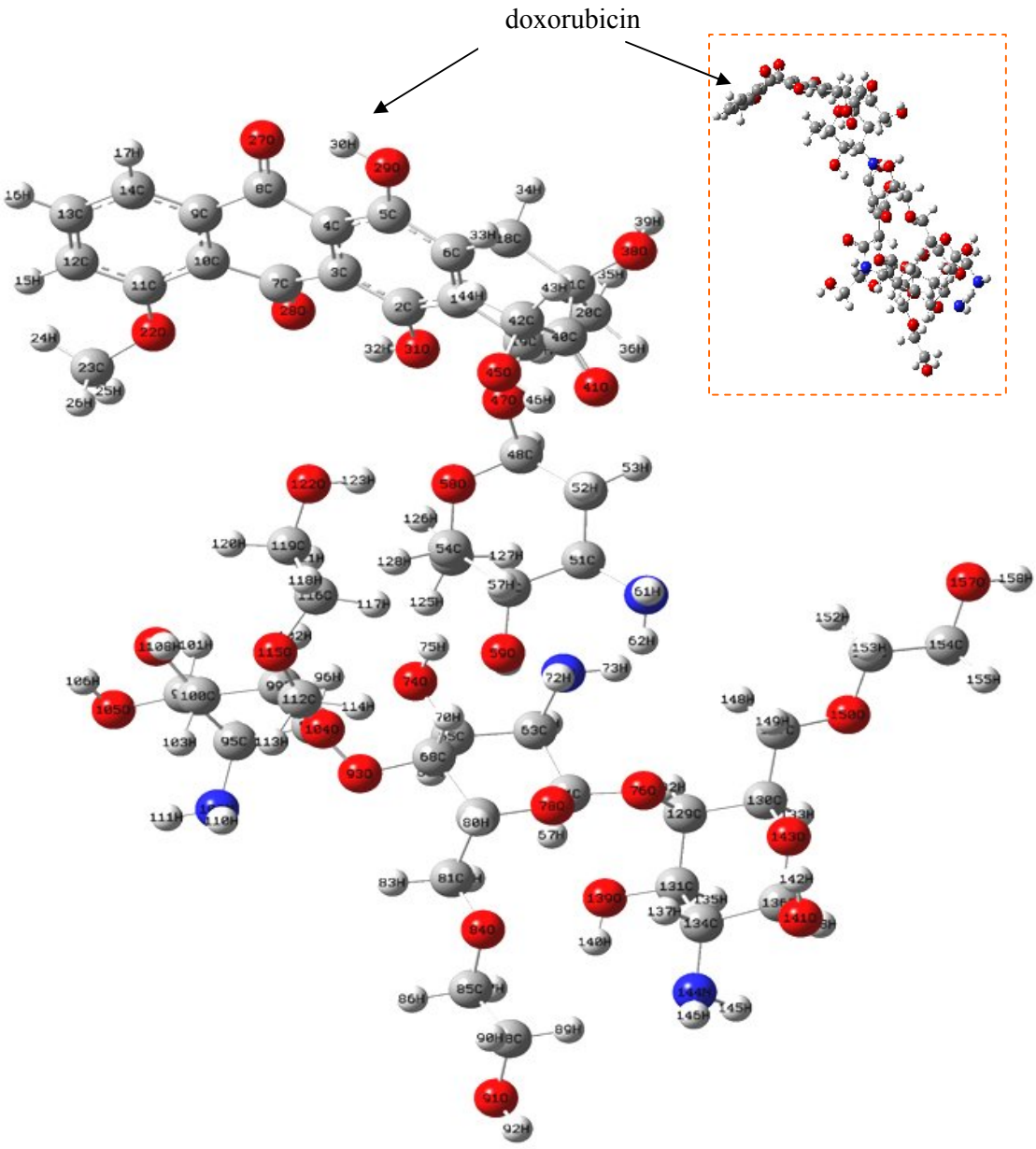

Figure 8a Molecular structure of doxorubicin and tri glucosamine-mono(ethylene glycol) by H-bond linkage (GC/DOX) from semi-empirical PM3 method

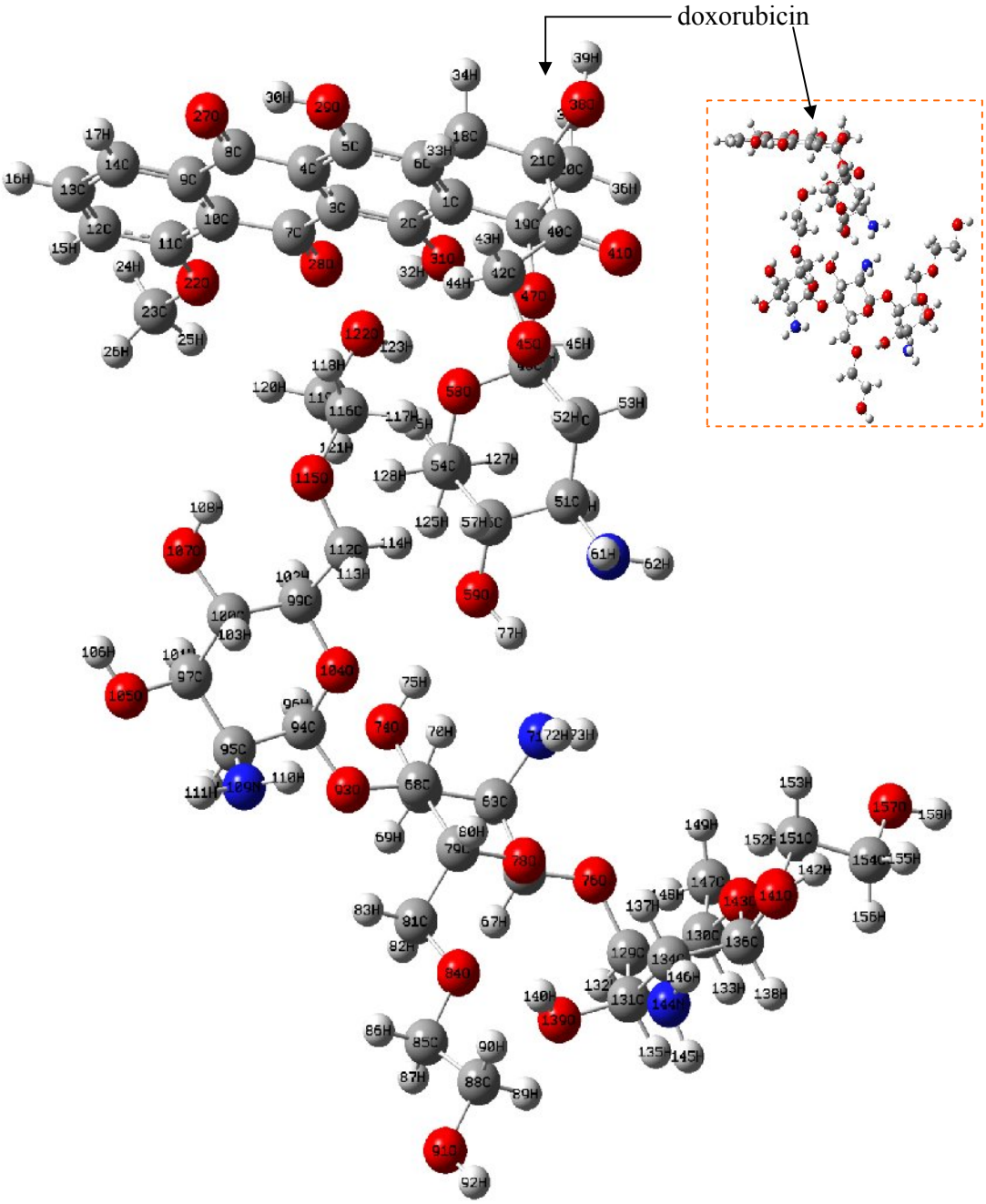

Figure 8b Molecular structure of doxorubicin and tri glucosamine-mono(ethylene glycol) by H-bond linkage (GC/DOX) from *ab initio* HF/6-31G method

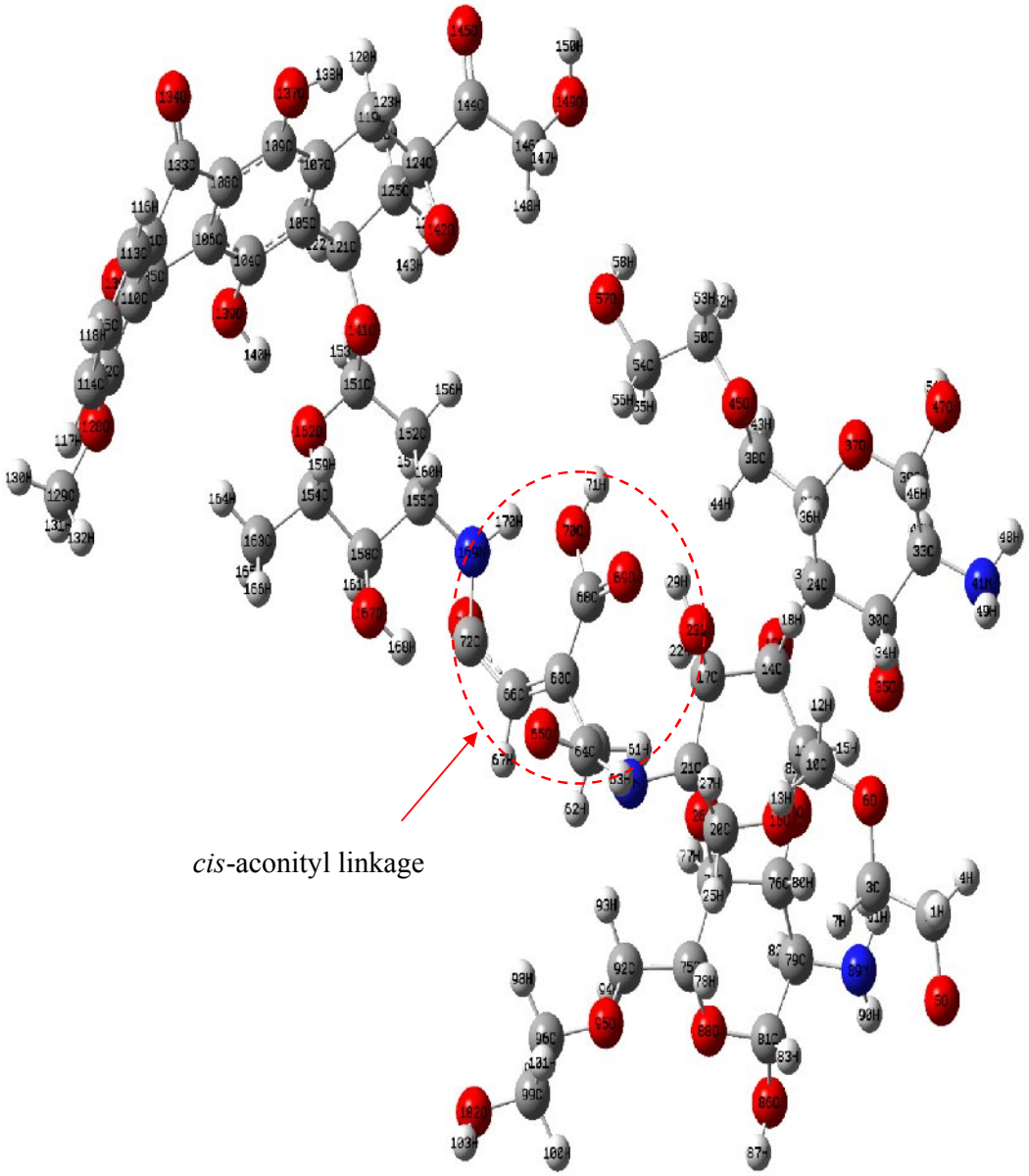

Figure 9a Molecular structure of doxorubicin and tri glucosamine-mono(ethylene glycol) by *cis*-aconityl linkage (GC-DOX) from semi-empirical PM3 method

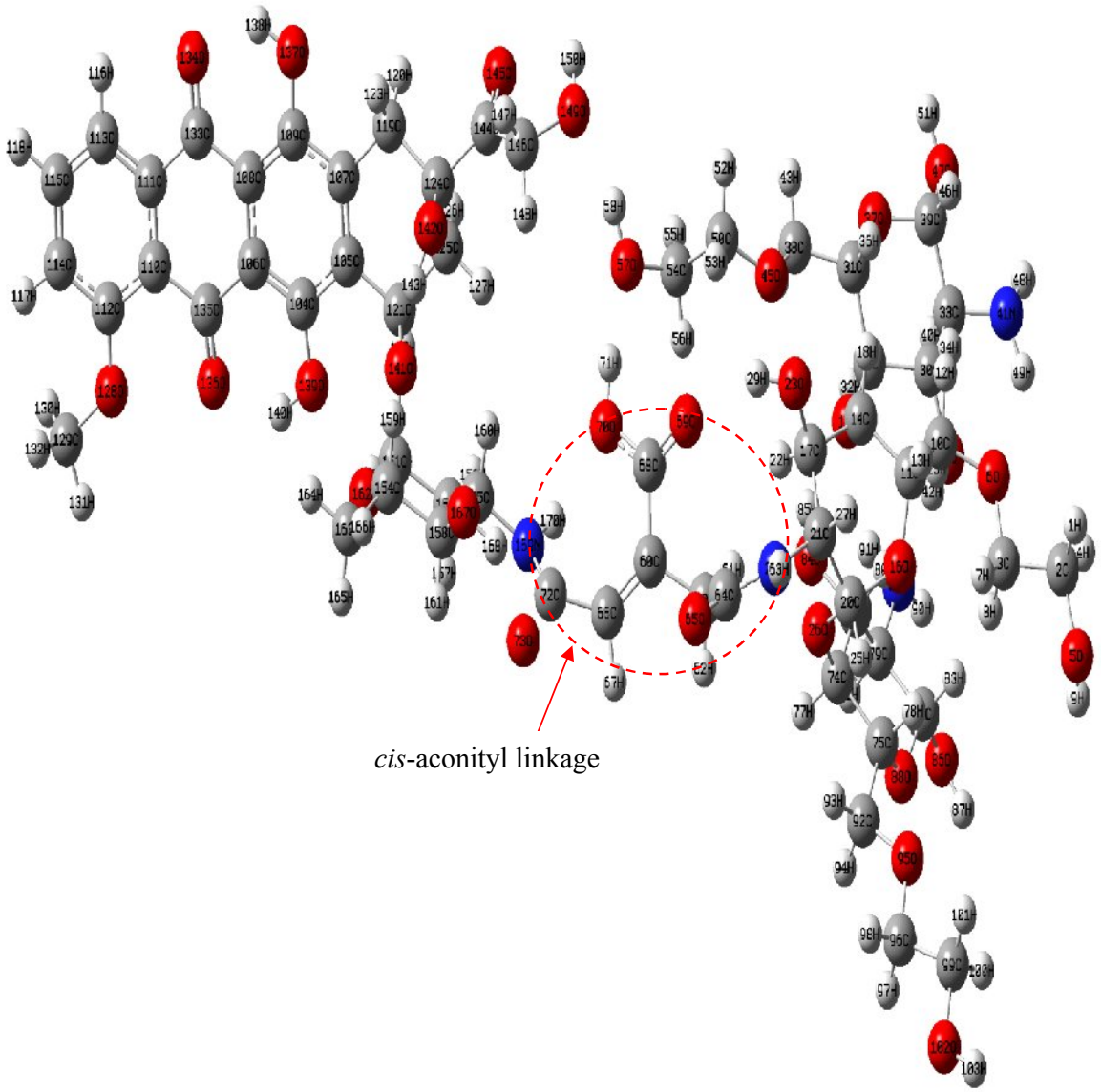

Figure 9b Molecular structure of doxorubicin and tri glucosamine-mono(ethylene glycol) by *cis*-aconityl linkage (GC-DOX) from *ab initio* HF/6-31G method

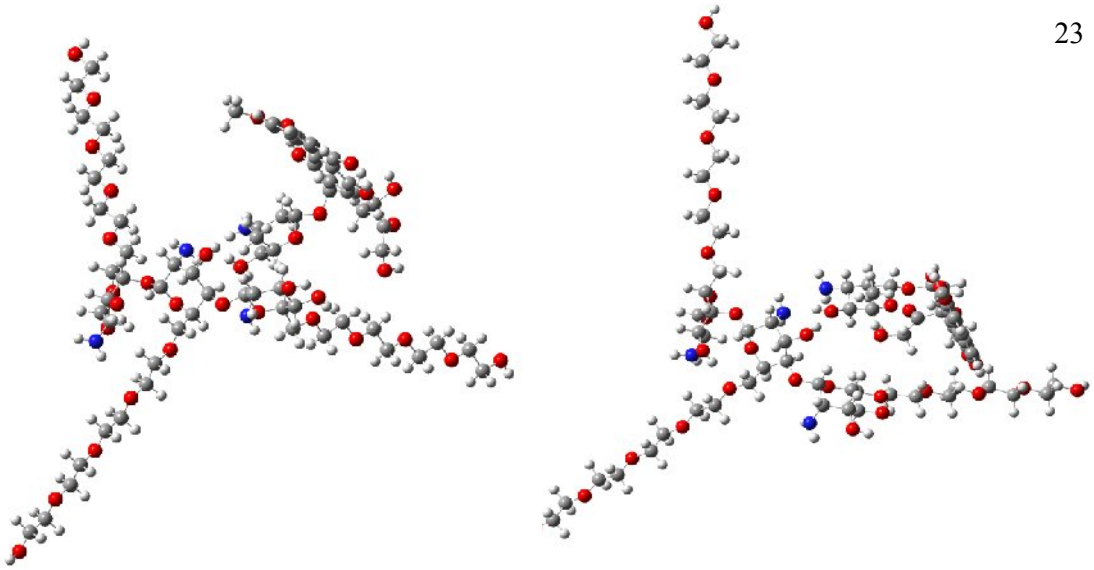

(a) (b)

Figure 10 Molecular structure of doxorubicin and tri glucosamine-quanta(ethylene glycol) by H-bond linkage from (a) semi-empirical PM3
(b) *ab initio* HF/6-31G method

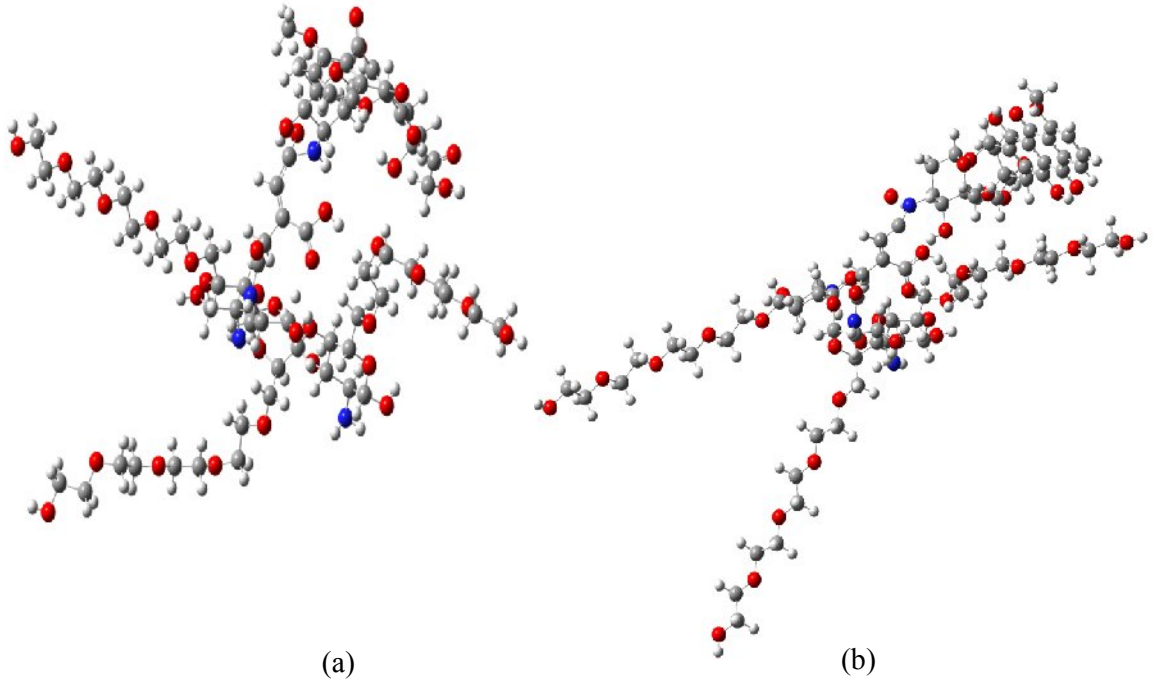

(a) (b)

Figure 11 Molecular structure of doxorubicin and tri glucosamine-quanta(ethylene glycol) by *cis*-aconityl linkage from (a) semi-empirical PM3
(b) *ab initio* HF/6-31G method

Molecular energy of GC/DOX and GC-DOX in optimization

The molecular optimization can be calculated from total molecular energy. The total energy of each molecule is decreased until reach optimum structure and then the total lowest molecular energy is obtained. The molecular energy of both GC/DOX and GC-DOX are calculated by B3LYP/6-31G method as shown in Table 2, and effect of ethylene glycol chain length to molecular formation is also investigated.

Table 2 The molecular energy of GC/DOX and GC-DOX structures by B3LYP/6-31G//PM3 and B3LYP/6-31G//HF/6-31G methods

Length of ethylene glycol	Molecular Energy (A.U.)			
	B3LYP/6-31G//PM3		B3LYP/6-31G//HF/6-31G	
	GC/DOX	GC-DOX	GC/DOX	GC-DOX
Mono-ethylene glycol	-4237.555	-4767.910	-4237.734	-4768.159
Di-ethylene glycol	-4698.891	-5229.235	-4699.082	-5229.489
Tri-ethylene glycol	-5160.238	-5690.576	-5160.426	-5690.846
Quanta-ethylene glycol	-5621.580	-6151.916	-5621.771	-6152.184
Penta-ethylene glycol	-6082.922	-6613.259	-6083.115	-6613.527

The molecular energy is calculated from the optimum product structure. From Table 2, it can be seen that the B3LYP/6-31G//HF/6-31G obtain molecular energies lower than B3LYP/6-3G//PM3. According to this result, the *ab initio* HF/6-31G method can optimize molecular structure better than semi-empirical PM3 method. However, the *ab initio* HF/6-31G method consumes rather long CPU time in optimization. For example, the optimized time of GC-DOX with mono(ethylene glycol) molecule by semi-empirical PM3 method is 27 minutes, but in *ab initio* HF/6-31G method is 8 days and 19.55 hours.

From this simulation, it can be seen that the molecular energies of GC-DOX structure are lower than GC/DOX. The stability of both GC/DOX and GC-DOX molecules are increased when length of ethylene glycol chain is increased. This can be concluded that the GC-DOX structures are more stable. Because the *cis*-aconityl linkage in GC-DOX molecule is able improve drug delivery system structures by forms bond between doxorubicin and glycol chitosan polymer. These simulation results correspond with reported from Kataoka *et al.* (2001). They concluded that in order to overcome the drug leakage limitation, drug had been chemically conjugated to polymer chains to improve the interaction between the drug and polymer.

The GC/DOX molecules have less stability because they form non-bond interaction between doxorubicin and glycol chitosan polymer. So, the following section will show how to interact between the doxorubicin and the glycol chitosan polymer by charge structure.

Charge structure in the GC/DOX molecule

In GC/DOX molecule, the interactions between drug and core domain of polymeric carrier rely on the balance of relatively weak interactions, such as hydrophobic, hydrogen bonding, and electrostatic interactions (Yokoyama *et al.,* 2000). Therefore, this section aims to study charge structure of doxorubicin and glycol chitosan polymer.

Charge of doxorubicin

The charge structure of doxorubicin by semi-empirical PM3 and *ab inito* HF/6-31G methods are shown in Figure 12.

The charge relates to electron density. The oxygen and nitrogen atom has a high electron density because these atoms have lone pair electron which to interact with other molecule. These atoms are negative charge while the low density such as

hydrogen atom is positive charge. The carbon atom can be positive or negative depending on dipole moment and electron density between atoms in molecule. In this simulation, the total charge of doxorubicin molecule is equal to zero. The negative charge of oxygen and nitrogen atoms can interact with positive charge atoms in other molecules.

(a)

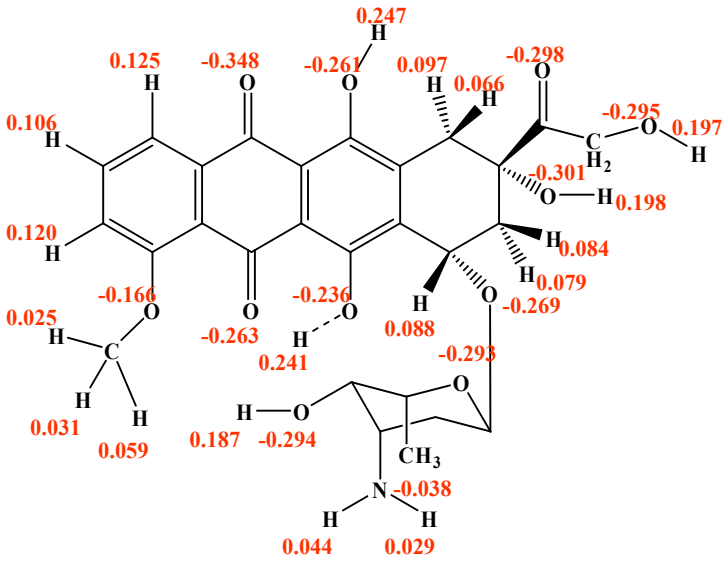

(b)

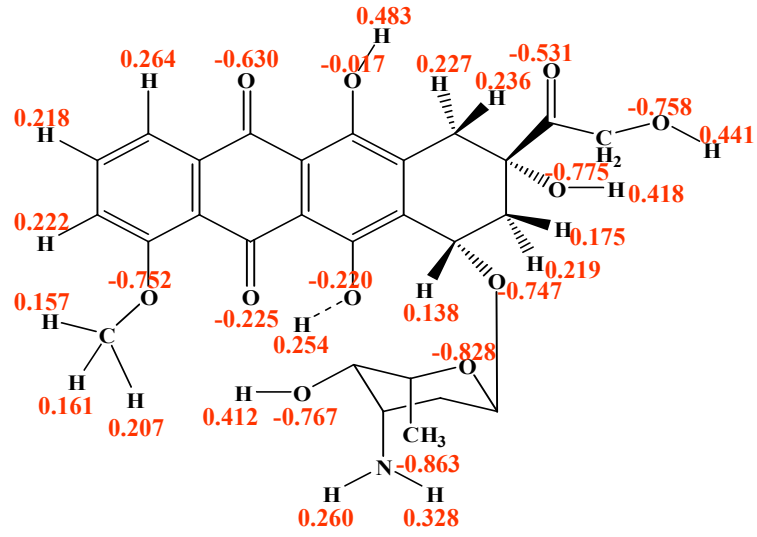

Figure 12 Charge of doxorubicin from optimization by (a) semi-empirical PM3 method (b) *ab initio* HF/6-31G method

Charge of glycol chitosan

The charge structure of glycol chitosan is studied by semi-empirical PM3 and *ab initio* HF/6-31G methods as shown in Figure 13.

(a)

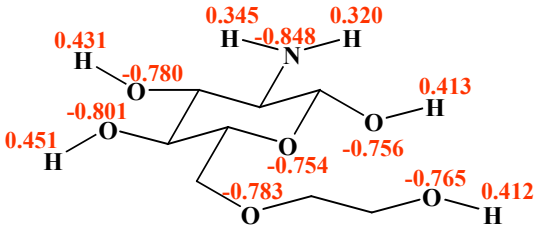

(b)

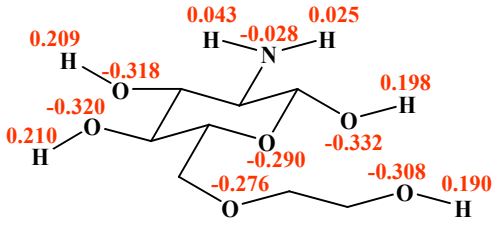

Figure 13 Charge of glycol chitosan from optimization by
(a) semi-empirical PM3 method (b) *ab initio* HF/6-31G method

The total charge of glycol chitosan molecule is equal to zero. From this simulation, the electron density of hydrogen atom which bonds with oxygen atom is lower than bonds with nitrogen atom. The oxygen atom can pull the electron more than nitrogen. These hydrogen atoms with low electron density, positive charge, can be bonded with the negative charge atoms such as oxygen and nitrogen atoms in doxorubicin molecules by electrostatic interaction (H-bond). Nevertheless, the H-bonding interaction is weak interaction. Accordingly, the GC/DOX molecules have stability less than GC-DOX molecules.

The results of charge structure simulation from two methods agree with experimental data from Janes *et al.* (2001). They modified the potential of chitosan nanoparticles carrying the anthracycline drug, doxorubicin. This drug can entrap a

cationic, hydrophilic molecule into nanoparticles formed by ionic elation of the positively charged polysaccharide chitosan. The experiment investigates the possibility of forming a complex between chitosan and doxorubicin prior to the formation of the particles. In consideration, the inherent polymer-drug is charge repulsion.

Bond length optimization

In molecular geometry, bond length or bond distance is the average distance between nuclei of two bonded atoms in a molecule. Bond length is inversely related to bond order, when more electrons participate in bond formation the bond will get shorter. Bond length is also inversely related to failing and bond strength and the bond dissociation energy, as a stronger bond is also a shorter bond.

The bond order is the number of electron pairs shared between two atoms in the formation of the bond. Bond order for C=C and C=O is 2. The amount of energy required to break a bond is called bond dissociation energy or simply bond energy. Since bond energies are consistent with bond lengths.

The bond length of the GC/DOX and GC-DOX with mono(ethylene glycol) from simulation by semi-empirical PM3 and *ab initio* HF/6-31G methods are shown in Tables 3 and 4, respectively. The bond length of H-bonding in GC/DOX molecules are shown in Figure 14.

The bond length of structure depends on electron density and dipole moment between atoms. If electron density and dipole moment increase, the bond length will decrease. From simulation, the length of delocalization bond is shorter than single bond but longer than double bond. For single bond, the bond lengths are C-C > C-N > C-O > C-H > N-H > O-H, due to the fact that the electron density of atoms are O > N > C > H. The higher electron density atoms can bond to the lower electron density atoms such as hydrogen and makes bond length shorter.

Table 3 Bond length of GC/DOX with mono(ethylene glycol) molecule (Figure 8) in ground state

Bond	PM3 (Å)	HF/6-31G (Å)
C23 – H24	1.100	1.081
C23 – O22	1.409	1.432
C11 – O22	1.375	1.353
C5 – O29	1.361	1.356
C48 – O58	1.417	1.435
C7 - C10	1.484	1.480
C1 – C19	1.509	1.507
C21 – C40	1.558	1.535
C51 – N60	1.479	1.457
O29 – H30	0.961	0.958
N60 – H61	0.999	0.998
C7 = O28	1.226	1.233
C11 = = C12	1.405	1.393
C63 – H66	1.117	1.081
C63 – C64	1.553	1.523
C63 – C65	1.554	1.535
C64 – O78	1.416	1.413
C65 – O74	1.403	1.402
C68 – O93	1.425	1.399
C81 – O84	1.420	1.425
C63 – N71	1.482	1.463
N71 – H72	1.005	0.999

Table 4 Bond length of GC-DOX with mono(ethylene glycol) molecule from Figure 9 in ground state

Bond	PM3 (Å)	HF/6-31G (Å)
C129 – H130	1.096	1.081
C129 – O128	1.406	1.432
C112 – O128	1.376	1.376
C109 – O137	1.366	1.356
C151 – O162	1.402	1.398
C110 - C135	1.494	1.479
C105 – C121	1.512	1.514
C124 – C144	1.551	1.513
C155 – N169	1.482	1.478
O137 – H138	0.952	0.958
N169 – H170	1.008	0.999
C135 = O136	1.211	1.231
C112 = = C114	1.404	1.393
C72 – N169	1.471	1.461
C60 = C66	1.351	1.335
C64 – N28	1.436	1.363
C21 – H27	1.130	1.079
C20 – C21	1.548	1.519
C17 – C21	1.548	1.536
C20 – O16	1.416	1.415
C17 – O23	1.417	1.424
C14 – O19	1.433	1.405
C10 – O6	1.408	1.422
C21 – N28	1.482	1.454
N41 – H48	0.998	0.995

Most bond lengths from optimization by *ab initio* HF/6-31G method from Tables 3 and 4 are shorter than semi-empirical PM3 method. Therefore, the molecular energies by *ab initio* HF/6-31G optimization are lower than the molecular energies by semi-empirical PM3 method.

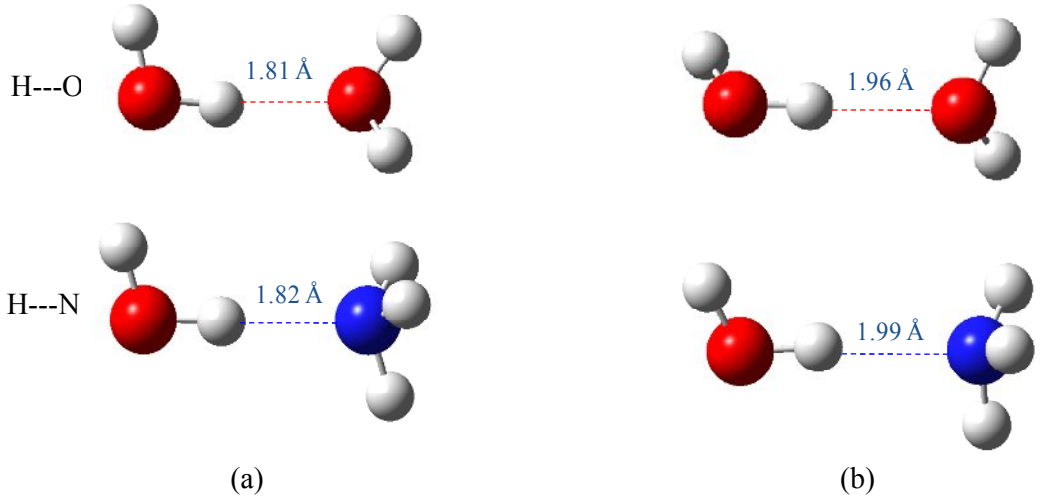

Figure 14 The bond length of H-bond in GC/DOX molecules
(a) semi-empirical PM3 method (b) *ab initio* HF/6-31G method

The interaction in GC/DOX molecules are electronic interaction or H-bond. The bond length of H-O bonding and H-N bonding as shown in Figure 14 are approximately at 1.8-1.9 Å. While the bond length between doxorubicin and glycol chitosan polymer in GC-DOX molecules in Table 4 are approximately at 1.3-1.4 Å. The shorter bond length has stronger than longer bond. From this bond length optimization, it can be concluded that the *cis-aconityl* linkage is used to improve the interaction between doxorubicin and glycol chitosan polymer by forms shorter bond than H-bond in GC/DOX molecules.

These geometrical parameters showed the reason why the GC-DOX structure is more stable than the GC/DOX structure which corresponds with many researches.

Kabanov *et al.,* (1996) studied about interaction between water-insuluble anti-cancer drugs and carriers. In most cases, anti-cancer drugs such as doxorubicin are incorporated into the hydrophobic core of micelles by hydrophobic interaction and/or electrostatic interaction. These interactions are weak between core of micelles and incorporated drugs. After injections of micellar solution, the loaded drugs in the core

of micelles are leaked by extreme dilutions by blood (Borovinskii and Khokhlov, 1998). Thus drug had been chemically conjugated to polymer chains to improve the interaction between drug and polymer (Kataoka *et al*., 2001).

Shen and Ryser (1981) studied the *cis*-aconityl linkage between daunomycin. *In vivo* test showed that N-*cis*-aconityl daunomycin-poly(D-lysine) entered cells and reached the lysosomal compartment, and that the *cis*-aconityl spacer releasesd daunomycin from poly(D-lysine) in the acidic environment of lysosomes.

Furthermore this simulation indicates the length of ethylene glycol chain (PEG) is increased, the molecular energy of both GC-DOX and GC/DOX is decreased. In other words, the drug carriers with increasing of polyethylene glycol chain are more stable. Since the compaction of the hydrophobic core interaction between doxorubicin and chitosan, the interaction of GC/DOX and GC-DOX molecules are stronger when PEG chain increasing. Ikuta *et al.* (2008) studied the characterization of polymeric carriers of doxorubicin and poly(*N-tert*-butylacrylamide) grafted chain poly(ethylene glycol) and Evans blue analogue. The polymeric carrier which contained a large number of PEG chains formed stable small particles. More PEG chains affected to tighten of core of micelle.

These simulation results and previous reports show that the *cis*-aconityl linkage can improve molecular structure of the doxorubicin carriers which resulting in bringing them to tumor cells efficiently without initial the burst drug release of loaded doxorubicin in blood vessel.

Next section will study doxorubicin release mechanism of *cis*-aconityl doxorubicin-glycol chitosan (GC-DOX) in acid and normal solutions and investigate the effect of length of ethylene glycol to released mechanism and glylcol chitosan degradation.

Doxorubicin release mechanism from GC-DOX molecules

Releasing of doxorubicin from the carrier system GC-DOX is associated with environment effect. Since this simulation studies the effect of solution on breaking bond between doxorubicin and *cis*-aconityl, two environments are provided to simulate. Hydronium ion (H_3O^+) is used as a model of acid condition and water (H_2O) is used as model of normal condition. The estimation of reaction can calculate from relative energy between total molecular energy of product and total molecular energy of reactant. The reaction optimization is firstly transition state optimized by semi-empirical PM3 and *ab initio* HF/6-31G method and then calculated the molecular energy of product structure of each step by B3LYP/6-31G method.

Acid condition

This section studies the reaction mechanism of GC-DOX in acid solution. The assumptions are 1) using one molecule of doxorubicin conjugated with tri glucosamine(ethylene glycol) via *cis*-aconityl represents GC-DOX as a model of conjugated drug delivery system and 2) using H_3O^+ (hydronium ion) represents acid condition.

This reaction has four continuous steps which are illustrated in Figure 15. In the first step, the hydronium ion tries to attract at bond between doxorubicin and *cis*-aconityl. The hydrogen atom in hydronium ion interacts with the nitrogen atom in doxorubicin called “transition state” in second step. In third step generates the doxorubicin, *cis*-aconityl cation and water in complex formation. Last step, the complex molecule from third step breakdown and then become three different molecules that are doxorubicin, *cis*-aconityl bonding with tri glucosamine(ethylene glycol) and water. This section also studies about effect of ethylene glycol chain length to drug release reaction. The relative energies from two methods are shown in Table 5. Figures 16 and 17 present the relative curves of doxorubicin release reactions in acid solution.

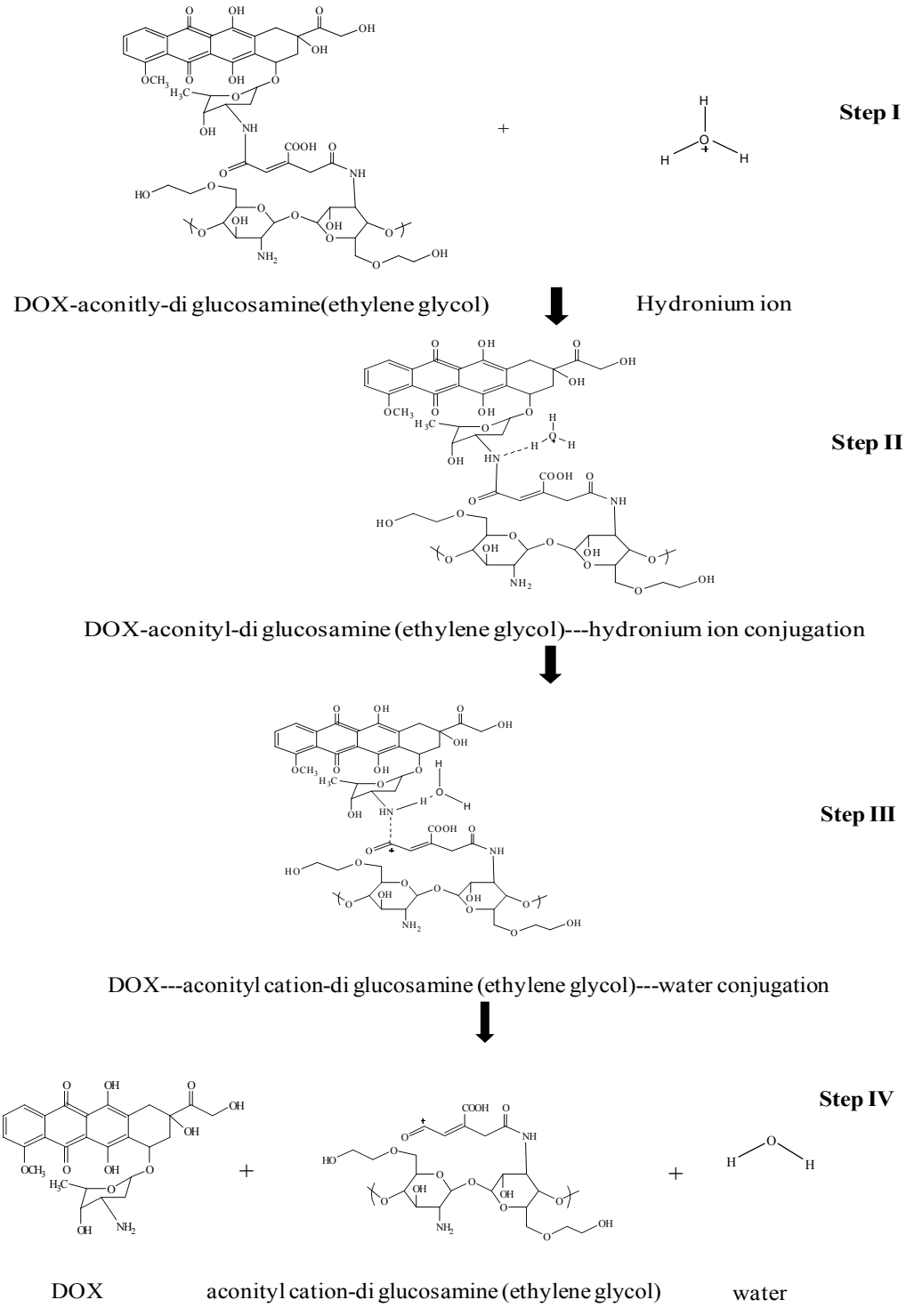

Figure 15 Reaction mechanism of doxorubicin release from GC-DOX in acid condition

Table 5 Relative energy of doxorubicin released mechanism from GC-DOX carrier in acid condition

Length of ethylene glycol	Reaction steps	Relative energy (kcal/mole)	
		B3LYP/6-31G //PM3	**B3LYP/6-31G //HF/6-31G**
Mono-ethylene glycol	Step I	0.00	0.00
	Step II	122.41	54.23
	Step III	-178.33	-43.11
	Step IV	-95.64	-77.84
Di-ethylene glycol	Step I	0.00	0.00
	Step II	119.27	109.28
	Step III	-174.49	-74.47
	Step IV	-113.31	-77.61
Tri-ethylene glycol	Step I	0.00	0.00
	Step II	160.18	219.98
	Step III	-153.68	71.63
	Step IV	-96.31	-69.53
Quanta-ethylene glycol	Step I	0.00	0.00
	Step II	222.22	980.49
	Step III	-126.11	171.48
	Step IV	-99.65	-73.39

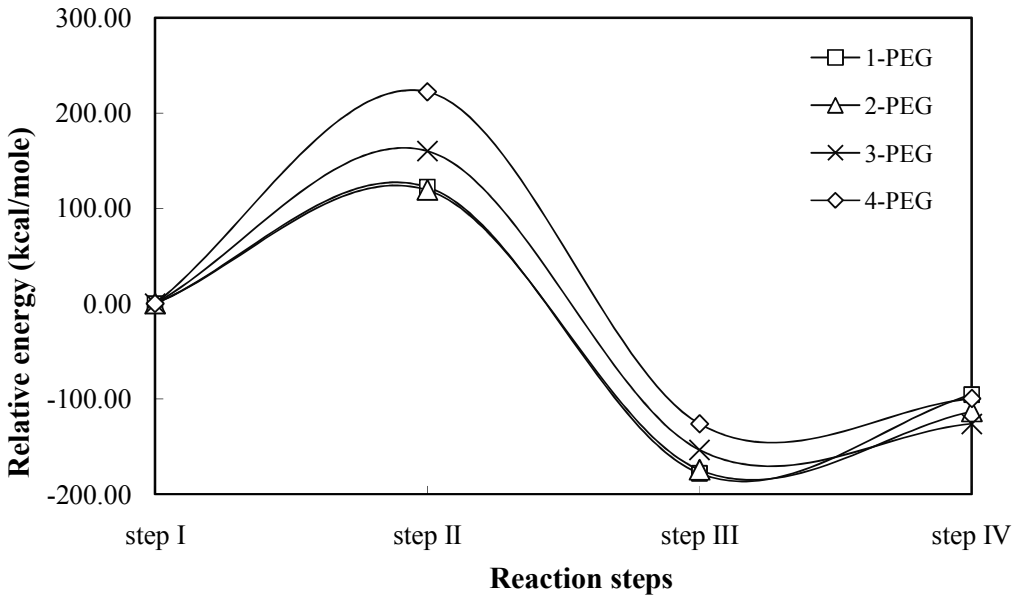

Figure 16 Relative energy curve of doxorubicin release from GC-DOX reaction in acid condition by B3LYP/6-31G//PM3 method

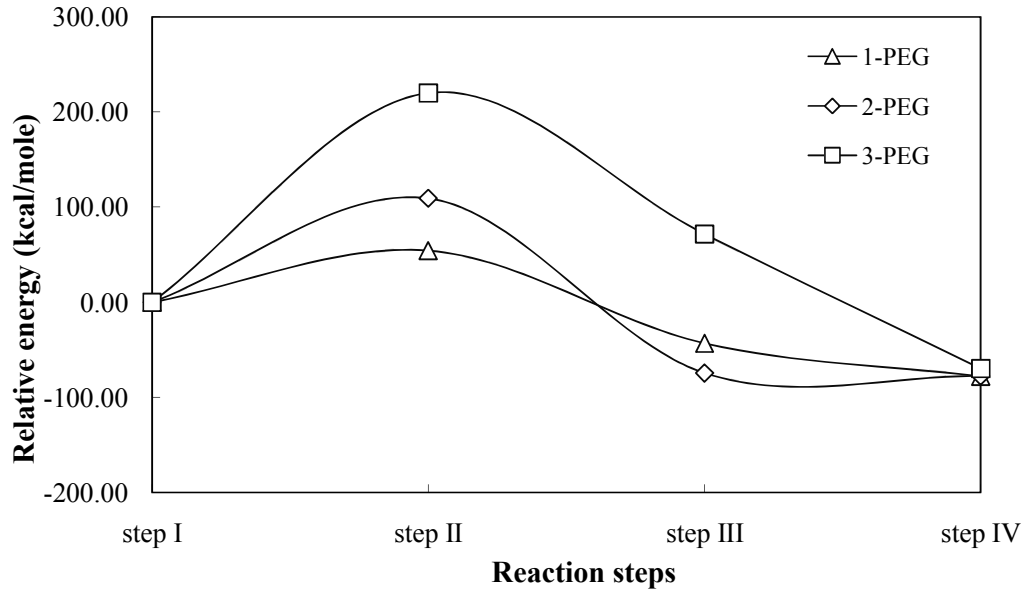

Figure 17 Relative energy curve of doxorubicin release from GC-DOX reaction in acid condition by B3LYP/6-31G//HF/6-31G method

The possibility of reaction is explained by relative energy of each reaction step. If relative energy of product is negative, the reaction has a possibility to occur. This reaction mechanism is simulated by B3LYP/6-31G//PM3 and B3LYP/6-31G//HF/6-31G methods. In step I, these molecules are the reactants. The relative energy in transition state is more than the step I because the hydronium ion needs some energy to react with doxorubicin and *cis*-aconitly bonding. This energy called activated energy.

The activated energies of doxorubicin release from each GC-DOX molecule in acid condition by B3LYP/6-31G//PM3 are 122.41, 119.27, 160.18 and 222.22 kcal/mol with mono, di, tri and quanta(ethylene glycol), respectively. The activated energies of this reaction by B3LYP/6-31G//HF/6-31G are 54.23, 109.28, 219.98 and 980.49 kcal/mole for mono, di, tri and quanta(ethylene glycol), respectively. Effect of length of ethylene glycol chain to drug and linkage bond breaking is less when it is short chain, not more than di(ethylene glycol). However, if ethylene glycol chain is more over, bond breaking is more difficult because high activated energy is needed to change the reactant to product. The polyethylene glycol (PEG) chain has steric hindrance effect which disturbs the hydronium ion to interact nitrogen atom in doxorubicin.

Normal condition

This section studies the reaction mechanism of GC-DOX in normal solution. The assumptions are 1) using one molecule of doxorubicin conjugated with tri glucosamine(ethylene glycol) by *cis*-aconityl represents GC-DOX system and 2) using H_2O represents acid condition. Releasing of doxorubicin from *cis*-aconityl linkage in normal condition has four continuous steps which are illustrated in Figure18.

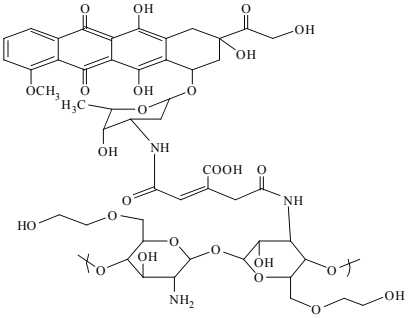

Step I

DOX-aconitly-di glucosamine(ethylene glycol) Water

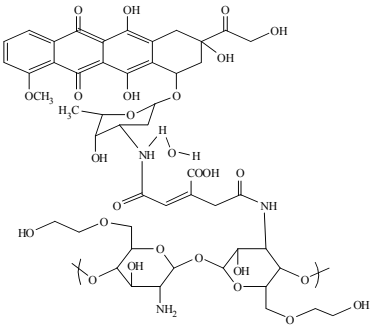

Step II

DOX-aconitly-di glucosamine(ethylene glycol)---water conjugation

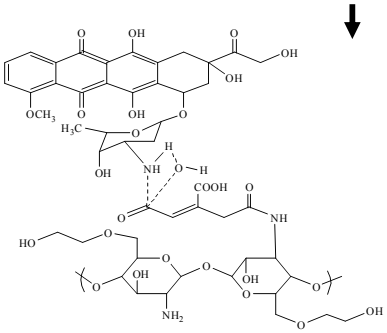

Step III

DOX---aconitly-di glucosamine(ethylene glycol) conjugation

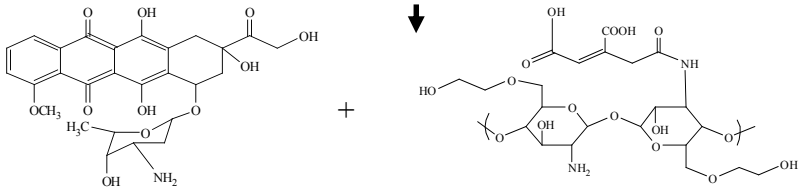

Step IV

DOX Aconitly-di glucosamine (ethylene glycol)

Figure 18 Reaction mechanism of doxorubicin release from GC-DOX in normal condition

In the first step, the water molecule (H_2O) attracts at the bond between doxorubicin and *cis*-aconityl. In second step, the hydrogen atom in water molecule interacts with the nitrogen atom in doxorubicin called "transition state". In step III generates the doxorubicin and *cis*-aconityl-tri glucosamine(ethylene glycol) in complex formation. Final step, the complex molecules separate from each other. There are two different molecules in final step that are doxorubicin and *cis*-aconityl-tri glucosamine(ethylene glycol). The relative energies of each reaction are shown in Table 6. Figures 19 and 20 show the relative curves of doxorubicin released mechanism in normal condition.

Table 6 Relative energy of doxorubicin released mechanism from GC-DOX carrier in acid condition

Length of ethylene glycol	**Reaction steps**	**Relative energy (kcal/mole)**	
		B3LYP/6-31G //PM3	**B3LYP/6-31G //HF/6-31G**
Mono-ethylene glycol	Step I	0.00	0.00
	Step II	379.06	387.94
	Step III	56.98	181.85
	Step IV	-93.70	-43.97
Di-ethylene glycol	Step I	0.00	0.00
	Step II	342.03	325.67
	Step III	39.78	162.17
	Step IV	-95.06	-58.54
Tri-ethylene glycol	Step I	0.00	0.00
	Step II	433.77	444.78
	Step III	34.68	113.24
	Step IV	-107.88	-50.78

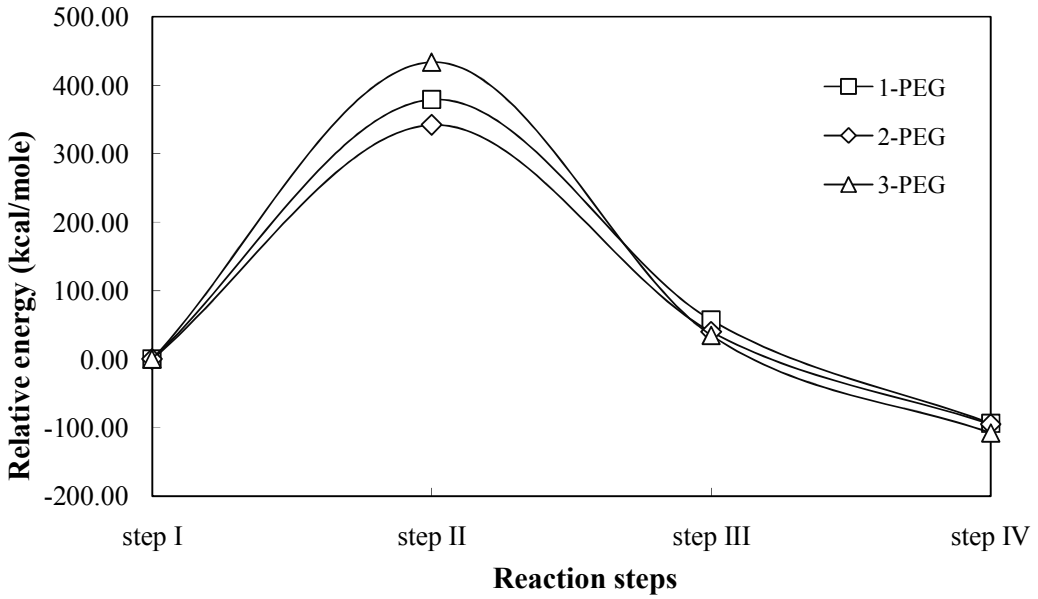

Figure 19 Relative energy curve of doxorubicin release from GC-DOX reaction in normal condition by B3LYP/6-31G//PM3 method

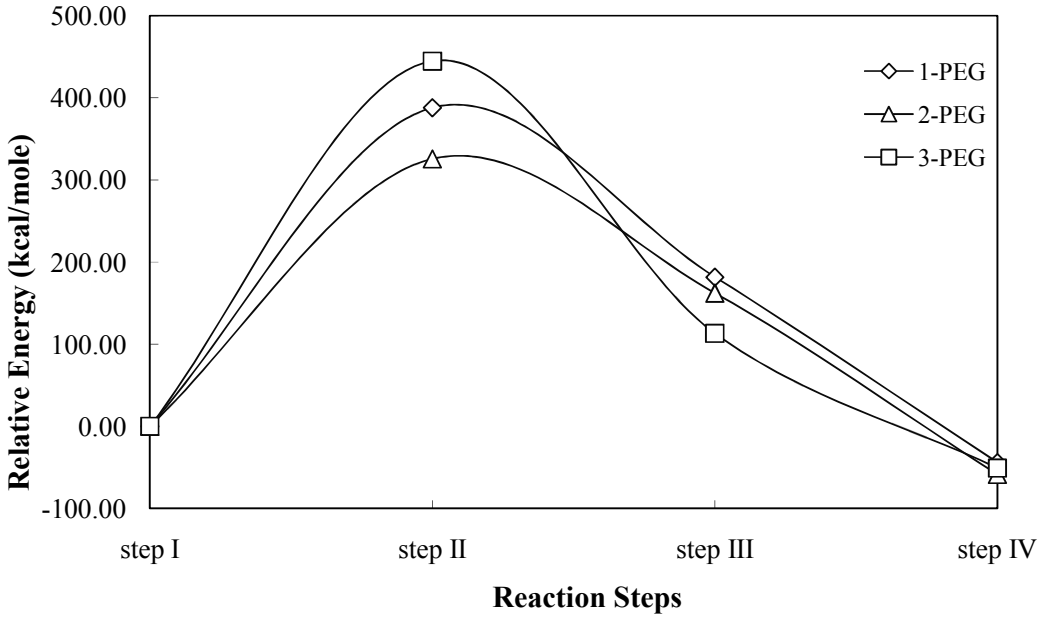

Figure 20 Relative energy curve of doxorubicin release from GC-DOX reaction in normal condition by B3LYP/6-31G//HF/6-31G method

The activated energies of doxorubicin releases from the GC-DOX in normal condition by B3LYP/6-31G//PM3 method are 379.06, 342.03 and 433.77 kcal/mole with mono, di and tri(ethylene glycol), respectively. The activated energies from B3LYP/6-31G//HF/6-31G method are 387.94, 325.67 and 444.78 kcal/mole. From the simulation by both semi-empirical PM3 and *ab initio* HF/6-31G methods of three reactions of doxorubicin releasing with mono-, di- and tri(ethylene glycol) in normal condition, it seems to be the activated energies are very high when compare with acid solution. The possibility of reaction which needs too high activated energy cannot occur. Consequently, *cis*-aconitly linkage cannot release the doxorubicin molecule from GC-DOX carrier in normal environment because this reaction needs a too high activated energy.

According to results in acid and normal conditions, these results correspond with experiment from Son *et al*., 2003. They studied doxorubicin released from DOX/GC-DOX in different pH media. Their report showed *cis*-aconityl linkage has pH-sensitive behavior with hydrolysis in an acidic environment. Doxorubicin was released continuously from nanoaggregated at pH 4, while the release of doxorubicin was almost negligible at pH 7. In blood stream is normal environment (pH 7.4) which has no effect with doxorubicin and linkage bonding. Since *cis*-aconityl has pH sensitive behavior and helps stable formation, it can control burst drug release in blood vessel before the drug carrier molecules to the target cells. When these drug carriers contact the target cell, they can release the drug by lysozyme from lysozome organells which work well in acid solution pH 4.5.

From the simulation of doxorubicin release mechanism in acid and normal conditions, it can indicate that the *cis*-aconityl linkage can release doxorubicin in acid solution, but doxorubicin is released hardly in normal solution.

Biodegradation of glycol chitosan

During doxorubicin releasing, glycol chitosan polymers will also degrade. So, this section will study about the bond breaking of glycol chitosan polymer by uses di-

glucosamine(ethylene glycol) represents glycol chitosan polymer. The reaction is in environment of acid and normal condition as well as in doxorubicin releasing. The estimation of reaction can calculate from relative energy between total molecular energy of product and total energy of reactant as same as previous section.

Acid condition

This section studies the effect of polymer bond breaking in acid solution. The assumptions are 1) using di-glucosamine(ethylene glycol) as a model of glycol chitosan polymer and 2) using H_3O^+ represents acid condition.

The reaction mechanism of di-glucosamine(ethylene glycol) bond breaking consists of four steps. There are reactant molecules, transition state and product molecules that are illustrated in Figure 21.

This reaction has four continuous steps. In the first step, the hydronium ion attracts di-glucosamine(ethylene glycol) at the polymer bond. The hydrogen atom in hydronium ion interacts with the oxygen atom of di glucosamine(ethylene glycol) called “transition state” in the second step. The molecules of di-glucosamine(ethylene glycol) and hydronium ion form a complex structure. In the third step, this reaction generates the glucosamine(ethylene glycol), glucosamine(ethylene glycol) cation, and water molecule in conjugated complex. Last step, the complex separates from each other. There are three different molecules in this final step; glucosamine(ethylene glycol) cation, glucosamine(ethylene glycol), and water. The relative energies of di - glucosamine(ethylene glycol) in acid solution by B3LYP/6-31G//PM3 and B3LYP/6-31G//HF/6-31G method are shown in Table 7 as the energy curves are shown in Figures 22 and 23.

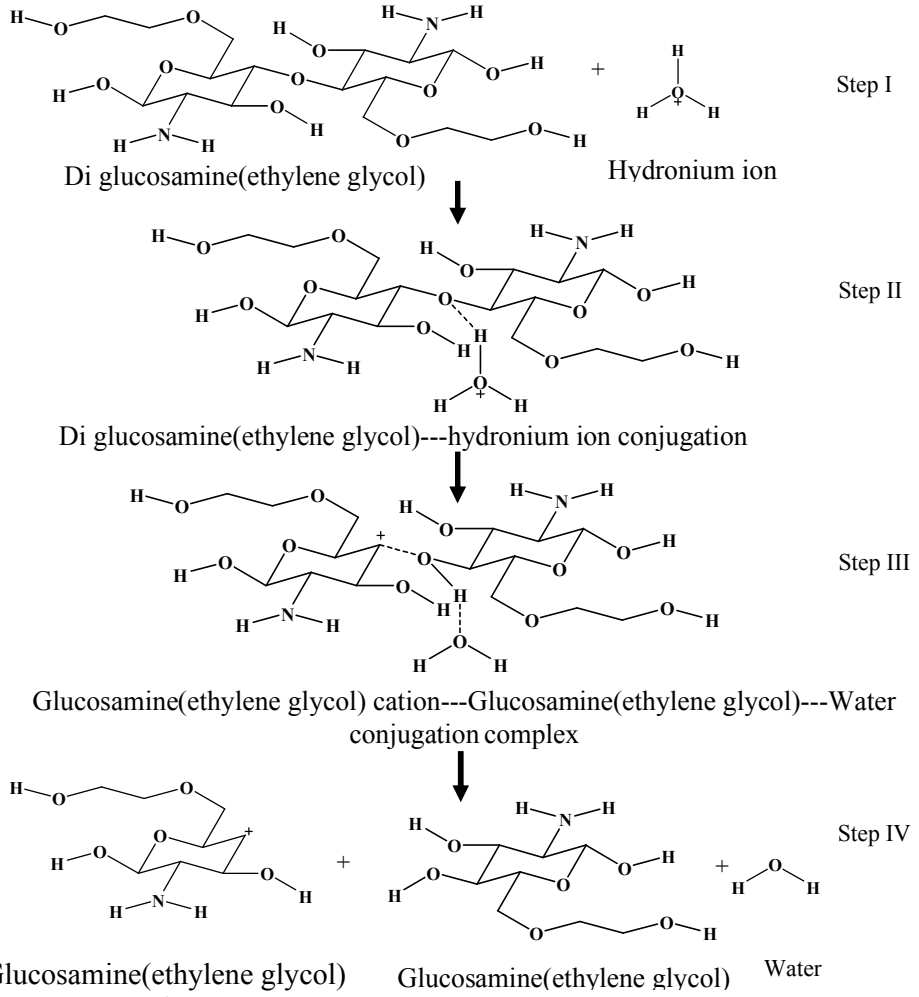

Figure 21 Reaction mechanism of di-glucosamine(ethylene glycol) in acid condition

Table 7 Relative energy of di-glucosamine(ethylene glycol) bond breaking in acid condition

Length of ethylene glycol	Reaction steps	Relative energy (kcal/mole)	
		B3LYP/6-31G //PM3	**B3LYP/6-31G //HF/6-31G**
Mono-ethylene glycol	Step I	0.00	0.00
	Step II	145.45	97.00
	Step III	-80.60	-42.63
	Step IV	-17.77	-13.41
Di-ethylene glycol	Step I	0.00	0.00
	Step II	91.12	62.59
	Step III	-72.65	-70.33
	Step IV	-16.60	-18.70
Tri-ethylene glycol	Step I	0.00	0.00
	Step II	61.41	44.11
	Step III	-72.07	-55.31
	Step IV	-6.61	-14.00
Quanta-ethylene glycol	Step I	0.00	0.00
	Step II	43.04	32.68
	Step III	-35.49	-53.86
	Step IV	-4.06	18.74
Penta-ethylene glycol	Step I	0.00	0.00
	Step II	33.63	35.31
	Step III	-50.21	-14.54
	Step IV	62.85	27.52

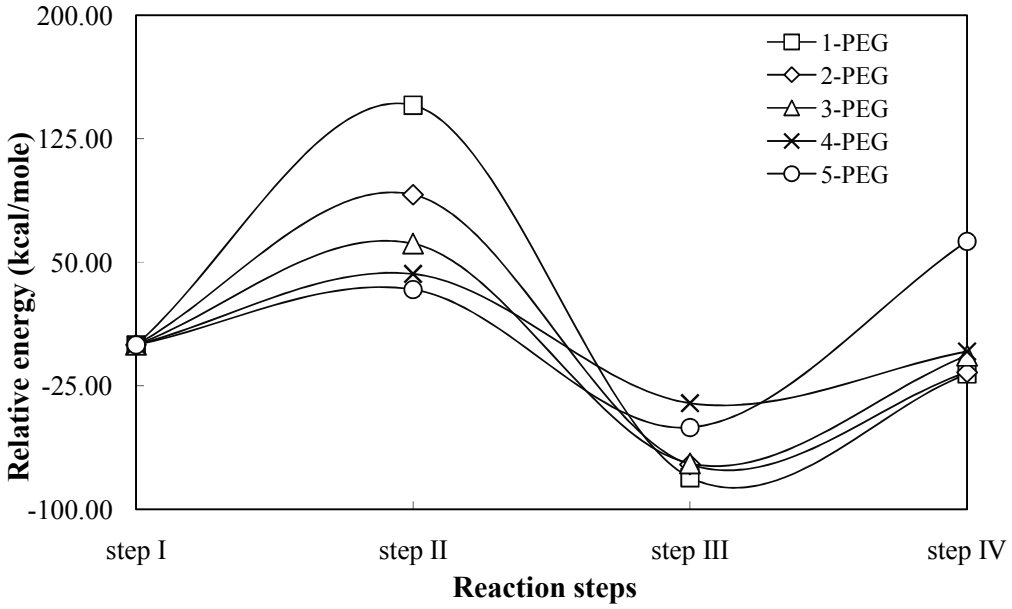

Figure 22 Relative energy curve of reaction mechanism of di-glucosamine(ethylene glycol) in acid condition by B3LYP/6-31G//PM3 method

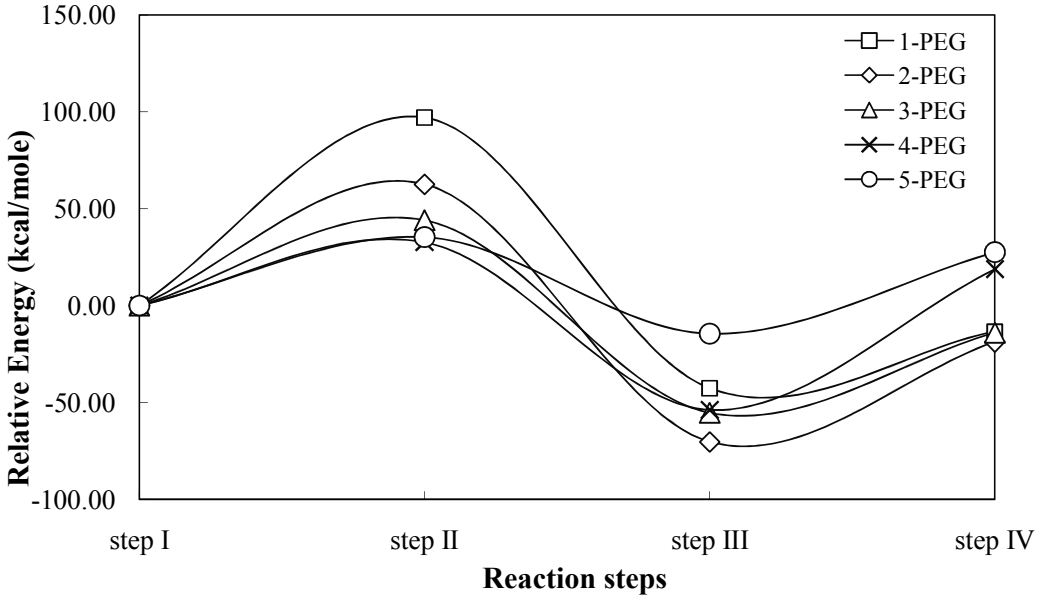

Figure 23 Relative energy curve of reaction mechanism of di-glucosamine(ethylene glycol in acid condition by B3LYP/6-31G//HF/6-31G method

The activated energies of reaction of di-glucosamine(ethylene glycol) in acid condition are 145.45, 91.12, 61.41, 43.04 and 33.63 kcal/mole for mono, di, tri, quanta and penta(ethylene glycol), respectively from B3LYP/6-31G//PM3 method. The activated energies from B3LYP/6-31G//HF/6-31G are 97.00, 62.59, 44.11, 32.31 and 35.31 kcal/mole for mono, di, tri, quanta and penta(ethylene glycol), respectively. Polyethylene glycol (PEG) has effect in glycol chitosan bond breaking. When the length of ethylene glycol chain is increased, it can decrease the activated energy of the reaction.

The simulation by semi-empirical PM3 method of bond breaking of di-glucosamine with mono, di, tri and quanta(ethylene glycol) have possibility to occur but di-glucosamine penta(ethylene glycol) cannot because the relative energy of the product is positive. Nevertheless, the reactions that have possibility to occur when simulate by *ab initio* HF/6-31G method are di-glucosamine with mono, di and tri(ethylene glycol) only, but for quanta- and penta(ethylene glycol) cannot occur.

Normal condition

This section studies the effect of polymer bond breaking in normal solution. The assumptions are 1) using di-glucosamine(ethylene glycol) as a model of glycol chitosan polymer and 2) using H_2O represents water condition.

The reaction mechanism of di-glucosamine(ethylene glycol) bond breaking consists of four steps. There are reactant molecules, transition state and product molecules that are illustrated in Figure 24.

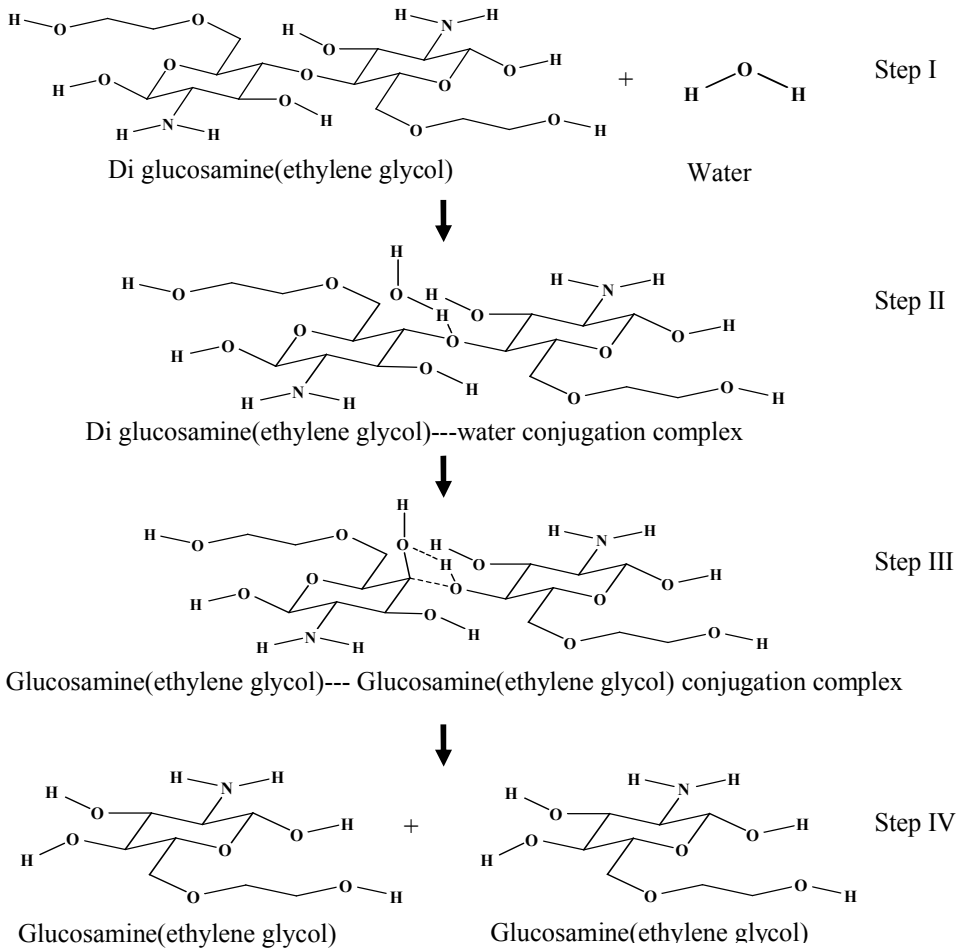

Figure 24 Reaction mechanism of di-glucosamine(ethylene glycol) in normal condition

This reaction contains four steps. Firstly, the water molecule attracts to di-glucosamine(ethylene glycol) at the polymer bond. Second step, the hydrogen atom in water molecule interacts with the oxygen atom in polymer bond of di-glucosamine(ethylene glycol), called this step "transition state". The lower electron density of hydrogen in water molecule is interacted from high electron density of oxygen atom in polymer bond and the oxygen of water interacts with carbon atom in one glucosamine molecule. The molecule of di glucosamine(ethylene glycol) and H_2O form complex structure. Final step, the glucosamine(ethylene glycol) molecule separate. The relative energies of di glucosamine(ethylene glycol) in water solution are shown in Table 8 as energy curves are shown in Figures 25 and 26.

Table 8 Relative energy of di-glucosamine(ethylene glycol) bond breaking reaction in normal condition

Length of ethylene glycol	Reaction steps	Relative energy (kcal/mole)	
		B3LYP/6-31G //PM3	**B3LYP/6-31G //HF/6-31G**
Mono-ethylene glycol	Step I	0.00	0.00
	Step II	456.92	474.96
	Step III	71.11	76.84
	Step IV	22.75	3.87
Di-ethylene glycol	Step I	0.00	0.00
	Step II	364.29	460.33
	Step III	96.29	64.30
	Step IV	17.71	3.05
Tri-ethylene glycol	Step I	0.00	0.00
	Step II	412.88	464.98
	Step III	96.11	74.65
	Step IV	14.70	2.69
Quanta-ethylene glycol	Step I	0.00	0.00
	Step II	409.54	451.65
	Step III	95.39	59.48
	Step IV	10.71	0.81

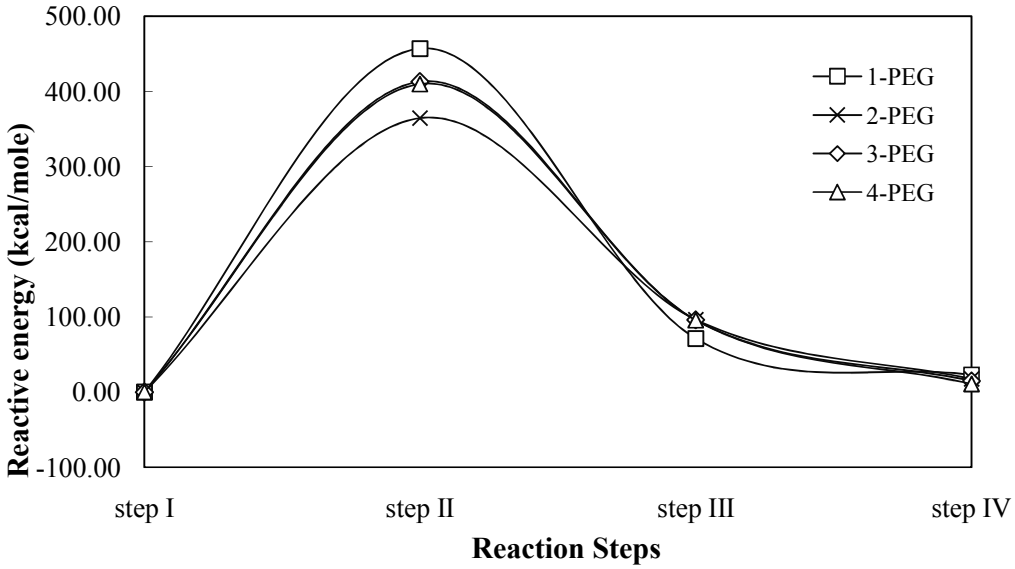

Figure 25 Relative energy curve of reaction mechanism of di-glucosamine(ethylene glycol) in normal condition by B3LYP/6-31G//PM3

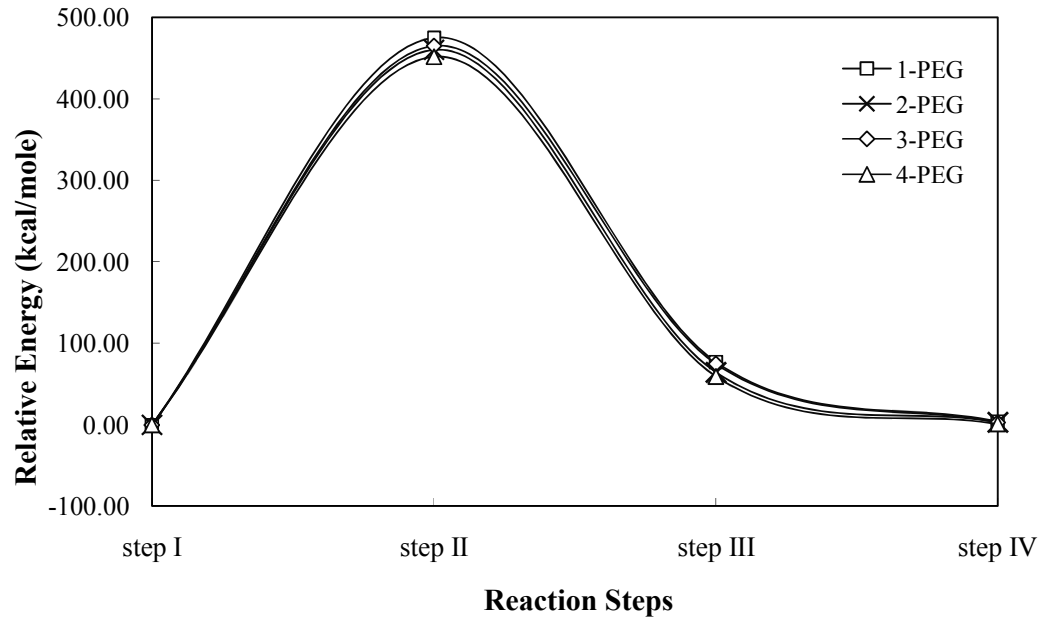

Figure 26 Relative energy curve of reaction mechanism of di-glucosamine(ethylene glycol) in normal condition by B3LYP/6-31G//HF/6-31G method

The activated energies from B3LYP/6-31G//PM3 simulation of the reactions in normal condition are 456.92, 364.29, 412.88 and 409.54 kcal/mole for mono, di, tri and quanta(ethylene glycol), respectively. The activated energies from B3LYP/6-31G//HF/6-31G are 474.96, 460.33, 464.98 and 451.65 kcal/mole for mono, di, tri and quanta(ethylene glycol), respectively. It can be seen that the glycol chitosan degradation in normal condition needs high activated energy as well as in doxorubicin release mechanism. The relative energies of the product molecules in every reaction which are obtained from these two methods in normal condition are positive. Therefore, the glycol chitosan degradation in normal solution cannot occur.

Oungbho and Muller in 1997 studied the degradation of chitosan capsule and reported that the chitosan capsule released drug at pH 1.2 faster than pH 7.4.

Therefore, the simulation result of degradation of glycol chitosan agrees well with the previous experiment data. Glycol chitosan polymer can be deformed easily in acid solution, but cannot in normal solution. The polyethylene glycol can decrease activated energy in the reaction. However, the reaction with longer polyethylene glycol chain, the product molecules are not stable. Consequently, the length of ethylene glycol chain which should be used is not more than tri(ethylene glycol).

The pathway of GC-DOX carriers when they are injected into blood vessel is represented in Figure 27. This pathway is modified from Kano *et al.* (2007). The loaded doxorubicin in GC-DOX carriers cannot release under pH 7.4 in blood vessel. When the GC-DOX carriers distribute to cancer cells, the endocytosis is a mechanism in order to transport the GC-DOX carriers in vesicles. These vesicles that contain GC-DOX carriers are permeated to endosome and reach to lysosome compartments. Doxorubicin molecules are released there by loysosomal enzyme which called lysozyme. The released doxorubicin molecules move to nucleus in order to inhibit growth of cancer cells. Some used drug carriers are degraded by lysozyme and then they are taken into vesicles again that called exocytosis to absolutely digest in other compartments. Finally, they are excreted from the body via kidneys in the urine or in the bile (Smith, 2005).

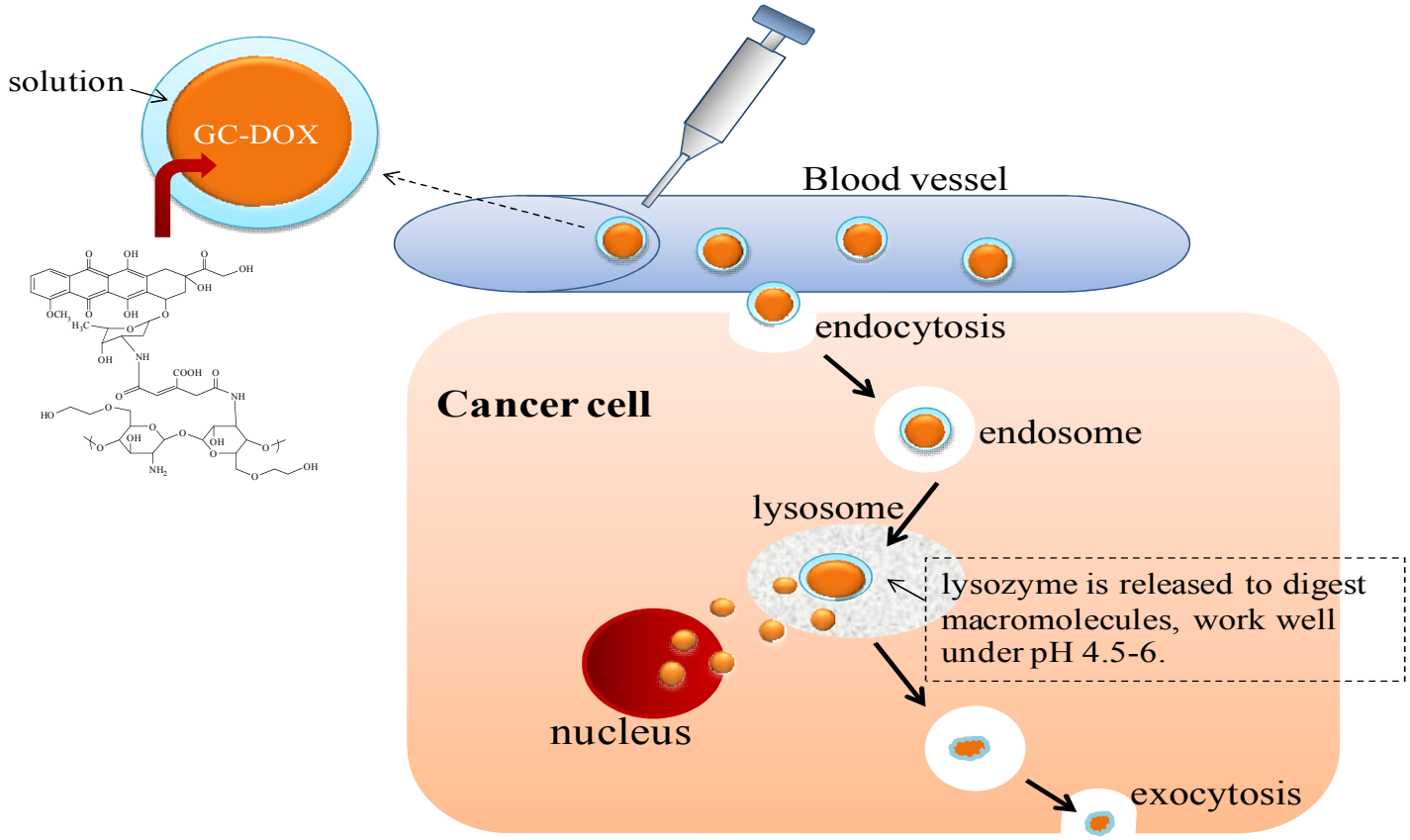

Figure 27 Pathway of GC-DOX carriers in the body

Source : Modified from Kano *et al.* (2007)

CONCLUSION

This thesis focused on the study of the conformation and drug release mechanism of drug delivery system of doxorubicin with glycol chitosan polymer by simulation. After comparing the molecular energy between the doxorubicin bonded glycol chitosan by H-bond (GC/DOX) and via *cis*-aconityl linkage (GC-DOX), it was found that molecular energy of the GC-DOX was lower than the GC/DOX. In the GC/DOX molecule, doxorubicin was loaded in glycol chitosan polymer by H-bonding which is a weak interaction. This bond could easily be deformed when it was injected into an intravenous blood vessel. The GC-DOX used *cis*-aconityl linkage to improve structure by bond forming that resulted in reducing of drug leakage by blood stream. The length of ethylene glycol chain increased the stability of the drug carrier due to the increase in the compaction of the hydrophobic core with the hydrophilic interaction.

The *cis*-aconityl linkage could release doxorubicin even under the environment effect. Doxorubicin was released well in acid condition. In the body, this condition occurs when the drug carrier reaches the target cell and then lysozyme, which is a digestive enzyme that works at pH 4.5, is released to digest the uncommon macromolecules. It can be seen from simulation results that the doxorubicin in GC-DOX cannot release in normal condition. Hence, it can be concluded that the GC-DOX can reduce the initial burst drug release after dilution by the blood vessel, because in blood vessel has neutral environment. Lysozyme is responsible for breakdown of polysaccharides. Therefore, glycol chitosan polymer can be degraded by this enzyme function as well.

The longer ethylene glycol chain has an effect on the need of high activated energy of doxorubicin release mechanism and it also makes the products of glycol chitosan degradation mechanism be unstable. Consequently, the suitable length of ethylene glycol chain is di(ethylene glycol) molecule.

RECOMMENDATIONS

1. The experimental laboratory of doxorubicin released reaction from GC-DOX molecule with various poly(ethylene glycol) chains should be studied and confirmed.

2. In order to approach the better results, more complex of the GC-DOX models, such as increasing the glycol chitosan polymer chain and more entrapping doxorubicin in hydrophobic space might need to be calculated.

3. Use higher method such as B3LYP or another molecular modeling or molecular dynamic programs to optimize the reaction mechanism.

4. In real situation, the drug released reaction occurs in liquid phase. Next simulation should be studied in liquid phase to closely approach the experimental data.

5. This simulation should be also observed in constant volume to calculate pH value in the system.

6. Distribution to tumor cells of drug carrier should be studied by simulation, because it is the goal of drug carrier to tumor cells.

LITERATURE CITED

Al-shankhani, A. and R. Duncan. 1999. Synthesis, controlled release properties and antitumur activity of alginate-cis-aconityl-daunomycin conjugates. **International Journal of Pharmaceutics.** 122:107-119**.**

Brannon-Peppas, L. and J.O. Blanchette**.** 2004. Nanoparticle and targeted systems for cancer therapy. **Advanced Drug Delivery Reviews.** 56: 1649-1659.

Chan, P. M., J. E.C. Kurisawa and Y. Yang. 2007. Synthesis and characterization of chitosan-g-poly(ethylene glycol)-folate as a non-viral carrier for tumor-targeted gene delivery. **Biomaterials.** 28: 540–549.

Cheng, J., B.A. Teply, I. Sherifi, J. Sung Gaurav, L. F.X. Gu, E. Levy-Nissenbaum, A.F. Radovic-Moren, R. Langer and O.C. Farokhzad. 2006. Formulation of functionalized PLGA–PEG nanoparticles for *in vivo* targeted drug delivery. **Biomaterials.** 28: 869–876.

Cummins, P.L. and J.E. Gready. 2003. Computational methods for the study of enzymic reaction mechanisms. II. An overlapping mechanically embedded method for hybrid semi-empirical-QM/MM calculations. **Journal of Molecular Structure: THEOCHEM**. 632(1-3): 247-257**.**

Frimand, K. and K.J. Jalkanen. 2002. SCC-TB, DFT/B3LYP, MP2, AM1, PM3 and RHF study of ethylene oxide and propylene oxide structures, VA and VCD spectra. **Chemical Physics.** 279: 161–178.

Foresman, J. and A. Frisch. 1996. **Exploring Chemistry with Electronic Structure Methods**, Second Edition. U.S.A.

Furgeson, D.Y., M.R. Dreher and A. Chilkoti. 2006. Structural optimization of a ‘‘smart’’ doxorubicin–polypeptide conjugate for thermally targeted delivery to solid tumors. **Journal of Controlled Release**. 110: 362 – 369.

Hu, F.Q., X.L. Wu, Y.Z. Du, J. You and H. Yuan. 2007. Cellular uptake and cytotoxicity of shell crosslinked stearic acid-grafted chitosan oligosaccharide micelles encapsulation doxorubicin. **Journal of Pharmaceutics and Biopharmaceutices.** 69: 117-125.

Ikuta, K., T. Mori, T. Yamanoto, T. Niidome, H. Shimokawa and Y. Katayama. 2008. Development of polymeric drug delivery system for recognizing vascular endothelial dysfunction. **Bioorganic & Medical Chemistry**. 16: 2811-2818.

Janes, K. A., M. P. Fresneau, A. Marazuela, A. Fabra and M. J. Alonso. 2001. Chitosan nanoparticles as delivery systems for doxorubicin. **Journal of Controlled Release.** 73: 255-267.

Kabonov, A.V., T.K. Bronich and V.A. Kabanov. 1996. Soluble stoichiometric complexes from poly (N-ethyl-4-vinylpyridinium) cations and poly(ethylene oxide)-block-polymethacrylate anions. **Macromolecules**. 29: 6797-6801.

Kano *et al*. 2007**. Improvement of cancer-targeting therapy, using nanocarriers for intractable solid toumors by inhibition of TGB-β singnaling.** Available Source: www.pnas.org/content/104/9/3460/suppl/DC1, February 16, 2007.

Kataoka, K., A. Harada, Y. Nagasaki. 2001. Block copolymer micelles for drug delivery: design, characterization and biological significance. **Advanced Drug Delivery Reviews.** 47: 113-131.

Khokhlov, A.R. and A.L. Brovinskii. 1998. Micelle formation in the dilute solution mixtures of block-copolymers. **Macromolecules** 31: 7636-7640.

Lam, Y., G. Goldbeck-wood and C. Boothirdoyd. 2004. Mesoscale Simulation and cryo-TEM of Nanoscale Drug Delivery Systems. **Molecular Simulation.** 30: 239-247.

Mitra, S., U. Gaur, P. C. Ghosh and A. N. Maitra. 2001. Tumour targeted delivery of encapsulated dextran–doxorubicin conjugate using chitosan nanoparticles as carrier. **Journal of Controlled Release.** 74: 317-323.

Nishiyama, N., Y. Kato, Y. Sugiyama, K. Kataoka. 2001. Cisplatin-loaded polymer-metal complex micelle with time-modulated decaying property as a novel drug delivery system. **Pharmaceutical Research**. 18: 1035-1041.

Oungbho, K., and B. W. Muller. 1997. Chitosan sponges as sustained release drug carriers. **International Journal of Pharmaceutics.** 156: 229-237.

Park, J. H., S. Kwon, M. Lee, H. Chung, J. Kim, Y. Kim, R. Park, I. Kim, S. B. Seo, I. C. Kwon and S. Y. Jeong. 2006. Self-assembled nanoparticles based on glycol chitosan bearing hydrophobic moieties as carriers for doxorubicin: *In vivo* biodistribution and anti-tumor activity. **Biomaterials.** 27: 119-126.

Remenyi, J., B. Balazs, S. Toth, A. Falus, G. Toth. and F. Hudecz. 2003. Isomer-dependent daunomycin release and in vitro antitumour effect of cis-aconityl-daunomycin. **Biochemical and Biophysical Research Communications**. 303 : 556–561.

Saito, K., T. Fujieda and H. Yoshioka. 2006. Feasibility of simple chitosan sheet as drug delivery carrier. **European Journal of Pharmaceutics and Biopharmaceutics.** 64(2): 161-166.

Shen, W. and H.J.P. Ryser. 1981. *Cis*-aconitly spacer between and macromolecular carriers: a model of pH-sensitive linkage released drug from a lysosomotropic conjugate. **Biochemical and Biophysical Research Communications**. 102: 1048-1054.

Smith, H. J. 2005. **Introduction to the Principles of Drug Design and Action**, Fourth Edition. U.S.A.

Son, Y.J., J. Jang, Y.W. Cho, H. Chung, R. Park, I.C. Kwon, I. Kim, J.Y. Park, S.B. Seo, C.R. Park and S.Y. Jeong. 2003. Biodistribution and anti-tumor efficacy of doxorubicin loaded glycol-chitosan nanoaggregates by EPR effect. **Journal of Controlled Release**. 91: 135–145.

Steinfeld, U., C. Pauli, N. Kaltz, C. Bergemannb and H. Lee. 2006. T lymphocytes as potential therapeutic drug carrier for cancer treatment. **International Journal of Pharmaceutics**. 311: 229–236.

Sun, G., J. Kürti, P. Rajczy, M. Kertesz, J. Hafner and G. Kresse. 2003. Performance of the Vienna ab initio simulation package (VASP) in chemical applications. **Journal of Molecular Structure (Theochem)**. 624: 37–45.

Thongjun, P. 2007. **Study of Doxorubicin in Glycol Chitosan Delivery by Molecular Modeling.** M.Eng. Thesis, Kasetsart University.

U.S. National library of medicine. 2007. **Doxorubicin. Medicine plus trusted health information for you.** Available source: http://www.nlm.nih.gov/ medlineplus/druginfo/medmaster/a682221.html, February 20, 2007.

Wikipedia. 2007. **Cancer**. Available Source: http://en.wikipedia.org/wiki/Cancer# Treatment of cancer, April 20, 2007.

Ye, Y.Q., F.L. Yang, F.Q. Hu, Y.Z. Du. and H.Y. Yu. 2008. Core-modified chitosan-based polymeric micelles for controlled release of doxorubicin. **International journal of pharmaceutics**. 352 : 294-301.

Yokoyama, M., K. Kataoka, T. Matsumoto, T. Okano, Y. Sakurai, S. Fukushima, K. Okamoto, G.S. Kwon. 2000. Doxorubicin-loaded poly(ethylene glycol)-poly (β-benzyl-L-aspartate) copolymer micelles : their pharmaceutical Characteristics and biological significance. **Journal of Control Release**. 64 : 143-153.

APPENDICES

Appendix A

Molecular energy

Appendix Table A1 The molecular energy from molecular optimization; Molecular Structure

Structure	Method	Molecular energy	
		(a.u.)	(kcal/mol)
Doxorubicin	B3LYP/6-31G//PM3	1,927.84	-1,209,740.76
	B3LYP/6-31G//HF/6-31G	-1,927.92	-1,209,786.65
Cis-aconityl	B3LYP/6-31G//PM3	-607.22	-381,035.54
	B3LYP/6-31G//HF/6-31G	-683.361	-428,815.75
Water (H_2O)	B3LYP/6-31G//PM3	-76.38	-47,932.31
	B3LYP/6-31G//HF/6-31G	-76.39	-47,932.95
Hydronium ion (H_3O^+)	B3LYP/6-31G//PM3	-76.68	-48,115.95
	B3LYP/6-31G//HF/6-31G	-76.68	-48,116.13
Mono glucosamine-mono(ethylene glycol)	B3LYP/6-31G//PM3	-820.82	-515,073.60
	B3LYP/6-31G//HF/6-31G	-820.85	-515,089.68
Di glucosamine-mono(ethylene glycol)	B3LYP/6-31G//PM3	-1,565.23	-982,195.49
	B3LYP/6-31G//HF/6-31G	-1,565.31	-982,250.27
Tri glucosamine-mono(ethylene glycol)	B3LYP/6-31G//PM3	-2,309.64	-1,449,324.92
	B3LYP/6-31G//HF/6-31G	-2,309.77	-1,449,403.83

Appendix Table A2 The molecular energy from molecular optimization; GC/DOX Structure

Structure	Method	Molecular energy	
		(a.u.)	(kcal/mol)
Doxorubicin-tri glucosamine-mono(ethylene glycol)	B3LYP/6-31G//PM3	-4,237.56	-2,659,108.42
Doxorubicin-tri glucosamine-mono(ethylene glycol)	B3LYP/6-31G//HF/6-31G	-4,237.73	-2,659,220.82
Doxorubicin-tri glucosamine-di(ethylene glycol)	B3LYP/6-31G//PM3	-4,698.89	-2,948,601.24
Doxorubicin-tri glucosamine-di(ethylene glycol)	B3LYP/6-31G//HF/6-31G	-4,699.08	-2,948,720.93
Doxorubicin-tri glucosamine-tri(ethylene glycol)	B3LYP/6-31G//PM3	-5,160.24	-3,238,100.91
Doxorubicin-tri glucosamine-tri(ethylene glycol)	B3LYP/6-31G//HF/6-31G	-5,160.43	-3,238,219.07
Doxorubicin-tri glucosamine-quanta(ethylene glycol)	B3LYP/6-31G//PM3	-5,621.58	-3,527,597.75
Doxorubicin-tri glucosamine-quanta(ethylene glycol)	B3LYP/6-31G//HF/6-31G	-5,621.77	-3,527,717.50
Doxorubicin-tri glucosamine-penta(ethylene glycol)	B3LYP/6-31G//PM3	-6,082.92	-3,817,094.58
Doxorubicin-tri glucosamine-penta(ethylene glycol)	B3LYP/6-31G//HF/6-31G	-6,083.12	-3,817,215.55

Appendix Table A3 The molecular energy from molecular optimization; GC-DOX Structure

Structure	Method	Molecular energy	
		(a.u.)	(kcal/mol)
Doxorubicin-tri glucosamine-mono(ethylene glycol)	B3LYP/6-31G//PM3	-4,767.91	-2,991,911.36
Doxorubicin-tri glucosamine-mono(ethylene glycol)	B3LYP/6-31G//HF/6-31G	-4,768.16	-2,992,067.40
Doxorubicin-tri glucosamine-di(ethylene glycol)	B3LYP/6-31G//PM3	-5,229.24	-3,281,397.53
Doxorubicin-tri glucosamine-di(ethylene glycol)	B3LYP/6-31G//HF/6-31G	-5,229.49	-3,281,556.89
Doxorubicin-tri glucosamine-tri(ethylene glycol)	B3LYP/6-31G//PM3	-5,690.58	-3,570,893.53
Doxorubicin-tri glucosamine-tri(ethylene glycol)	B3LYP/6-31G//HF/6-31G	-5,691.00	-3,571,161.72
Doxorubicin-tri glucosamine-quanta(ethylene glycol)	B3LYP/6-31G//PM3	-6,151.92	-3,860,388.86
Doxorubicin-tri glucosamine-quanta(ethylene glycol)	B3LYP/6-31G//HF/6-31G	-6,152.18	-3,860,556.92
Doxorubicin-tri glucosamine-penta(ethylene glycol)	B3LYP/6-31G//PM3	-6,613.26	-4,149,886.10
Doxorubicin-tri glucosamine-penta(ethylene glycol)	B3LYP/6-31G//HF/6-31G	-6,613.53	-4,150,054.09

Appendix Table A4 The molecular energy from molecular optimization; Glycol Chitosan Polymer Structure

Structure	Method	Molecular energy	
		(a.u.)	(kcal/mol)
Di glucosamine-mono(ethylene glycol)	B3LYP/6-31G//PM3	-1,565.23	-982,195.49
Di glucosamine-mono(ethylene glycol)	B3LYP/6-31G//HF/6-31G	-1,565.31	-982,250.27
Di glucosamine-di(ethylene glycol)	B3LYP/6-31G//PM3	-1,872.79	-1,175,193.80
Di glucosamine-di(ethylene glycol)	B3LYP/6-31G//HF/6-31G	-1,872.88	-1,175,248.83
Di glucosamine-tri(ethylene glycol)	B3LYP/6-31G//PM3	-2,180.35	-1,368,191.82
Di glucosamine-tri(ethylene glycol)	B3LYP/6-31G//HF/6-31G	-2,180.44	-1,368,247.69
Di glucosamine-quanta(ethylene glycol)	B3LYP/6-31G//PM3	-2,487.91	-1,561,189.67
Di glucosamine-quanta(ethylene glycol)	B3LYP/6-31G//HF/6-31G	-2,488.00	-1,561,247.08
Di glucosamine-penta(ethylene glycol)	B3LYP/6-31G//PM3	-2,795.47	-1,754,187.86
Di glucosamine-penta(ethylene glycol)	B3LYP/6-31G//HF/6-31G	-2,795.57	-1,754,245.31

Appendix B

Relative energy of doxorubicin released mechanism from GC-DOX carrier with solution effects

Appendix Table B1 The relative energy of doxorubicin released mechanism of GC-DOX with mono(ethylene glycol) in acid solution

Reaction step	Molecular energy (kcal/mol)			Total energy (kcal/mol)	Relative energy (kcal/mol)
Simulation by B3LYP/6-31G//PM3 method					
Reactant	DOX-acontityl-tri glucosamine-mono(ethylene glycol)	H_3O^+			
	-2,991,911.36	-48,115.95		-3,040,027.32	0.00
Reactant complex	DOX-acontityl-tri glucosamine-mono(ethylene glycol)--H_3O^+				
	-3,039,904.90			-3,039,904.90	122.41
Product complex	DOX--- acontityl-tri glucosamine-mono(ethylene glycol) cation---H_2O				
	-3,040,205.65			-3,040,205.65	-178.33
Product	acontityl-tri glucosamine-mono(ethylene glycol) cation	DOX	H_2O		
	-1,782,449.89	-1,209,740.76	-47,932.31	-3,040,122.96	-95.64
Simulation by B3LYP/6-31G//HF-6-31G method					
Reactant	DOX-acontityl-tri glucosamine-mono(ethylene glycol)	H_3O^+			
	-3,040,183.53	-48,116.13		-3,040,183.53	0.00
Reactant complex	DOX-acontityl-tri glucosamine-mono(ethylene glycol)--H_3O^+				
	-3,040,129.30			-3,040,129.30	54.23
Product complex	DOX--- acontityl-tri glucosamine-mono(ethylene glycol) cation---H_2O				
	-3,040,226.64			-3,040,226.64	-43.11
Product	acontityl-tri glucosamine-mono(ethylene glycol) cation	DOX	H_2O		
	-1,782,541.78	-1,209,786.65	-47,932.95	-3,040,261.37	-77.84

Appendix Table B2 The relative energy of doxorubicin released mechanism of GC-DOX with di(ethylene glycol) in acid solution

Reaction step	Molecular energy (kcal/mol)			Total energy (kcal/mol)	Relative energy (kcal/mol)
Simulation by B3LYP/6-31G//PM3 method					
Reactant	DOX-aconityl-tri glucosamine-di(ethylene glycol)	H_3O^+			
	-3,281,397.53	-48,115.95		-3,329,513.48	0.00
Reactant complex	DOX-aconityl-tri glucosamine-di(ethylene glycol)--H_3O^+				
	-3,329,394.21			-3,329,394.21	119.27
Product complex	DOX--- aconityl-tri glucosamine-di(ethylene glycol) cation---H_2O				
	-3,329,687.97			-3,329,687.97	-174.49
Product	aconityl-tri glucosamine-di(ethylene glycol) cation	DOX	H_2O		
	-2,071,953.72	-1,209,740.76	-47,932.31	-3,329,626.79	-113.31
Simulation by B3LYP/6-31G//HF-6-31G method					
Reactant	DOX-aconityl-tri glucosamine-tri(ethylene glycol)	H_3O^+			
	-3,281,556.89	-48,116.13		-3,329,673.02	0.00
Reactant complex	DOX-aconityl-tri glucosamine-tri(ethylene glycol)--H_3O^+				
	-3,329,563.74			-3,329,563.74	109.28
Product complex	DOX--- aconityl-tri glucosamine-tri(ethylene glycol) cation---H_2O				
	-3,329,747.49			-3,329,747.49	-74.47
Product	aconityl-tri glucosamine-tri (ethylene glycol) cation	DOX	H_2O		
	-2,072,031.04	-1,209,786.65	-47,932.95	-3,329,750.63	-77.61

Appendix Table B3 The relative energy of doxorubicin released mechanism of GC-DOX with tri(ethylene glycol) in acid solution

Reaction step	Molecular energy (kcal/mol)			Total energy (kcal/mol)	Relative energy (kcal/mol)
Simulation by B3LYP/6-31G//PM3 method					
Reactant	DOX-aconityl-tri glucosamine-tri(ethylene glycol)	H_3O^+			
	-3,570,893.53	-48,115.95		-3,619,009.49	0.00
Reactant complex	DOX-aconityl-tri glucosamine-tri(ethylene glycol)--H_3O^+				
	-3,618,849.30			-3,618,849.30	160.18
Product complex	DOX--- aconityl-tri glucosamine-tri(ethylene glycol) cation---H_2O				
	-3,619,163.17			-3,619,163.17	-153.68
Product	aconityl-tri glucosamine-tri (ethylene glycol) cation	DOX	H_2O		
	-2,361,432.72	-1,209,740.76	-47,932.31	-3,619,105.79	-96.31
Simulation by B3LYP/6-31G//HF-6-31G method					
Reactant	DOX-aconityl-tri glucosamine-tri(ethylene glycol)	H_3O^+			
	-3,571,062.75	-48,116.13		-3,619,178.88	0.00
Reactant complex	DOX-aconityl-tri glucosamine-tri(ethylene glycol)--H_3O^+				
	-3,618,958.90			-3,618,958.90	219.98
Product complex	DOX--- aconityl-tri glucosamine-tri(ethylene glycol) cation---H_2O				
	-3,619,107.25			-3,619,107.25	71.63
Product	aconityl-tri glucosamine-tri (ethylene glycol) cation	DOX	H_2O		
	-2,361,528.82	-1,209,786.65	-47,932.95	-3,619,248.41	-69.53

Appendix Table B4 The relative energy of doxorubicin released mechanism of GC-DOX with quanta(ethylene glycol) in acid solution

Reaction step	Molecular energy (kcal/mol)			Total energy (kcal/mol)	Relative energy (kcal/mol)
Simulation by B3LYP/6-31G//PM3 method					
Reactant	DOX-acontityl-tri glucosamine-quanta(ethylene glycol)	H_3O^+			
	-3,860,388.86	-48,115.95		-3,908,504.82	0.00
Reactant complex	DOX-acontityl-tri glucosamine-quanta(ethylene glycol)--H_3O^+				
	-3,908,282.59			-3,908,282.59	222.22
Product complex	DOX--- acontityl-tri glucosamine-quanta(ethylene glycol) cation---H_2O				
	-3,908,630.92			-3,908,630.92	-126.11
Product	aconityl-tri glucosamine-quanta(ethylene glycol) cation	DOX	H_2O		
	-2,650,931.40	-1,209,740.76	-47,932.31	-3,908,604.47	-99.65
Simulation by B3LYP/6-31G//HF-6-31G method					
Reactant	DOX-acontityl-tri glucosamine-quanta(ethylene glycol)	H_3O^+			
	-3,860,556.92	-48,116.13		-3,908,673.05	0.00
Reactant complex	DOX-acontityl-tri glucosamine-quanta(ethylene glycol)--H_3O^+				
	-3,907,692.55			-3,907,692.55	980.49
Product complex	DOX--- acontityl-tri glucosamine-quanta(ethylene glycol) cation---H_2O				
	-3,908,501.57			-3,908,501.57	171.48
Product	aconityl-tri glucosamine-quanta(ethylene glycol) cation	DOX	H_2O		
	-2,651,026.85	-1,209,740.76	-47,932.95	-3,908,746.44	-73.39

Appendix Table B5 The relative energy of doxorubicin released mechanism of GC-DOX with mono(ethylene glycol) in normal solution

Reaction step	Molecular energy (kcal/mol)		Total energy (kcal/mol)	Relative energy (kcal/mol)
Reactant	DOX-acontityl-tri glucosamine-mono(ethylene glycol)	H_2O		
	-2,991,911.36	-47,932.31	-3,039,843.67	0.00
Reactant complex	DOX-acontityl-tri glucosamine-mono(ethylene glycol)-- H_2O			
	-3,039,464.62		-3,039,464.62	379.06
Product complex	DOX--- acontityl-tri glucosamine-mono(ethylene glycol)			
	-3,039,786.69		-3,039,786.69	56.98
Product	acontityl-tri glucosamine-mono(ethylene glycol)	DOX		
	-1,830,196.62	-1,209,740.76	-3,039,937.38	-93.70
Simulation by B3LYP/6-31G//HF-6-31G method				
Reactant	DOX-acontityl-tri glucosamine-mono(ethylene glycol)	H_2O		
	-2,992,067.40	-47,932.95	-3,040,000.34	0.00
Reactant complex	DOX-acontityl-tri glucosamine-mono(ethylene glycol)-- H_2O			
	-3,039,612.40		-3,039,612.40	387.94
Product complex	DOX--- acontityl-tri glucosamine-mono(ethylene glycol)			
	-3,039,818.49		-3,039,818.49	181.85
Product	acontityl-tri glucosamine-mono(ethylene glycol)	DOX		
	-1,830,279.93	-1,209,764.39	-3,040,044.31	-43.97

Appendix Table B6 The relative energy of doxorubicin released mechanism of GC-DOX with di(ethylene glycol) in normal solution

Reaction step	Molecular energy (kcal/mol)		Total energy (kcal/mol)	Relative energy (kcal/mol)
Reactant	DOX-acontityl-tri glucosamine-di(ethylene glycol)	H_2O		
	-3,281,397.53	-47,932.31	-3,329,329.84	0.00
Reactant complex	DOX-acontityl-tri glucosamine-di(ethylene glycol)-- H_2O			
	-3,328,987.81		-3,328,987.81	342.03
Product complex	DOX--- acontityl-tri glucosamine-di(ethylene glycol)			
	-3,329,290.06		-3,329,290.06	39.78
Product	acontityl-tri glucosamine-di(ethylene glycol)	DOX		
	-2,119,684.14	-1,209,740.76	-3,329,424.90	-95.06
Simulation by B3LYP/6-31G//HF-6-31G method				
Reactant	DOX-acontityl-tri glucosamine-di(ethylene glycol)	H_2O		
	-3,281,556.89	-47,932.95	-3,329,489.83	0.00
Reactant complex	DOX-acontityl-tri glucosamine-di(ethylene glycol)-- H_2O			
	-3,329,164.16		-3,329,164.16	325.67
Product complex	DOX--- acontityl-tri glucosamine-di(ethylene glycol)			
	-3,329,327.66		-3,329,327.66	162.17
Product	acontityl-tri glucosamine-di(ethylene glycol)	DOX		
	-2,119,783.99	-1,209,764.39	-3,329,548.37	-58.54

Appendix Table B7 The relative energy of doxorubicin released mechanism of GC-DOX with tri(ethylene glycol) in normal solution

Reaction step	Molecular energy (kcal/mol)		Total energy (kcal/mol)	Relative energy (kcal/mol)
Reactant	DOX-acontityl-tri glucosamine-tri(ethylene glycol)	H_2O		
	-3,570,893.53	-47,932.31	-3,618,825.84	0.00
Reactant complex	DOX-acontityl-tri glucosamine-tri(ethylene glycol)-- H_2O			
	-3,618,392.07		-3,618,392.07	433.77
Product complex	DOX--- acontityl-tri glucosamine-tri(ethylene glycol)			
	-3,618,791.16		-3,618,791.16	34.68
Product	acontityl-tri glucosamine-tri(ethylene glycol)	DOX		
	-2,409,192.96	-1,209,740.76	-3,618,933.72	-107.88
Simulation by B3LYP/6-31G//HF-6-31G method				
Reactant	DOX-acontityl-tri glucosamine-tri(ethylene glycol)	H_2O		
	-3,571,062.75	-47,932.95	-3,618,995.69	0.00
Reactant complex	DOX-acontityl-tri glucosamine-tri(ethylene glycol)-- H_2O			
	-3,618,550.91		-3,618,550.91	444.78
Product complex	DOX--- acontityl-tri glucosamine-tri(ethylene glycol)			
	-3,618,882.45		-3,618,882.45	113.24
Product	acontityl-tri glucosamine-tri(ethylene glycol)	DOX		
	-2,409,282.09	-1,209,764.39	-3,619,046.48	-50.78

Appendix C

Relative energy of glycol chitosan polymer bond breaking with solution effects

Appendix Table C1 The relative energy of bond breaking of Di glucosamine-mono(PEG) in acid solution.

Reaction step	Molecular energy (kcal/mol)			Total energy (kcal/mol)	Relative energy (kcal/mol)
Simulation by B3LYP/6-31G//PM3 method					
Reactant	Di glucosamine-mono(PEG)	H_3O^+			
	-982,195.49	-48,115.95		-1,030,311.45	0.00
Reactant complex	Di glucosamine-mono(PEG)--H_3O^+				
	-1,030,165.99			-1,030,165.99	145.45
Product complex	Glucosamine-mono(PEG) cation---Glucosamine-mono(PEG)---H_2O				
	-1,030,392.05			-1,030,392.05	-80.60
Product	Glucosamine-mono(PEG) cation	Glucosamine-mono(PEG)	H_2O		
	-467,323.31	-515,073.60	-47,932.31	-1,030,329.22	-17.77
Simulation by B3LYP/6-31G//HF-6-31G method					
Reactant	Di glucosamine-mono(ethylene glycol)	H_3O^+			
	-982,250.27	-48,116.13		-1,030,366.40	0.00
Reactant complex	Di glucosamine-mono(PEG)--H_3O^+				
	-1,030,269.40			-1,030,269.40	97.00
Product complex	Glucosamine-mono(PEG) cation---Glucosamine-mono(PEG)---H_2O				
	-1,030,409.03			-1,030,409.03	-42.63
Product	Glucosamine-mono(PEG) cation	Glucosamine-mono(PEG)	H_2O		
	-467,357.18	-515,089.68	-47,932.95	-1,030,379.81	-13.41

Appendix Table C2 The relative energy of bond breaking of Di glucosamine-di(PEG) in acid solution

Reaction step	Molecular energy (kcal/mol)			Total energy (kcal/mol)	Relative energy (kcal/mol)
Simulation by B3LYP/6-31G//PM3 method					
Reactant	Di glucosamine-di(PEG)	H_3O^+			
	-1,175,197.33	-48,115.95		-1,223,313.28	0.00
Reactant complex	Di glucosamine-di(PEG)--H_3O^+				
	-1,223,222.16			-1,223,222.16	91.12
Product complex	Glucosamine-di(PEG) cation---Glucosamine-di(PEG)---H_2O				
	-1,223,385.93			-1,223,385.93	-72.65
Product	Glucosamine-di(PEG) cation	Glucosamine-di(PEG)	H_2O		
	-563,822.74	-611,574.83	-47,932.31	-1,223,329.88	-16.60
Simulation by B3LYP/6-31G//HF-6-31G method					
Reactant	Di glucosamine-di(PEG)	H_3O^+			
	-1,175,248.83	-48,115.95		-1,223,364.79	0.00
Reactant complex	Di glucosamine-di(PEG)--H_3O^+				
	-1,223,302.20			-1,223,302.20	62.59
Product complex	Glucosamine-di(ethylene glycol) cation---Glucosamine-di(ethylene glycol)---H_2O				
	-1,223,435.12			-1,223,435.12	-70.33
Product	Glucosamine-di(PEG) cation	Glucosamine-di(PEG)	H_2O		
	-563,861.14	-611,586.85	-47,932.95	-1,223,383.49	-18.70

Appendix Table C3 The relative energy of bond breaking of Di glucosamine-tri(PEG) in acid solution

Reaction step	Molecular energy (kcal/mol)			Total energy (kcal/mol)	Relative energy (kcal/mol)
Simulation by B3LYP/6-31G//PM3 method					
Reactant	Di glucosamine-tri(PEG)	H_3O^+			
	-1,368,191.82	-48,115.95		-1,416,307.78	0.00
Reactant complex	Di glucosamine-tri(PEG)--H_3O^+				
	-1,416,246.37			-1,416,246.37	61.41
Product complex	Glucosamine-tri(PEG) cation---Glucosamine-tri(PEG)---H_2O				
	-1,416,379.85			-1,416,379.85	-72.07
Product	Glucosamine-di(PEG) cation	Glucosamine-di(PEG)	H_2O		
	-660,308.17	-708,073.90	-47,932.31	-1,416,314.39	-6.61
Simulation by B3LYP/6-31G//HF-6-31G method					
Reactant	Di glucosamine-tri(PEG)	H_3O^+			
	-1,368,247.69	-48,115.95		-1,416,363.65	0.00
Reactant complex	Di glucosamine-tri(PEG)--H_3O^+				
	-1,416,319.53			-1,416,319.53	44.11
Product complex	Glucosamine-tri(PEG) cation---Glucosamine-tri(PEG)---H_2O				
	-1,416,418.96			-1,416,418.96	-55.31
Product	Glucosamine-di(ethylene glycol) cation	Glucosamine-di(ethylene glycol)	H_2O		
	-660,355.73	-708,088.97	-47,932.95	-1,416,377.64	-14.00

Appendix Table C4 The relative energy of bond breaking of Di glucosamine-quanta(PEG) in acid solution

Reaction step	Molecular energy (kcal/mol)			Total energy (kcal/mol)	Relative energy (kcal/mol)
Simulation by B3LYP/6-31G//PM3 method					
Reactant	Di glucosamine-quanta(PEG)	H_3O^+			
	-1,561,189.67	-48,115.95		-1,609,305.63	0.00
Reactant complex	Di glucosamine-quanta(PEG)--H_3O^+				
	-1,609,262.59			-1,609,262.59	43.04
Product complex	Glucosamine-quanta(PEG) cation---Glucosamine-quanta(PEG)---H_2O				
	-1,609,341.12			-1,609,341.12	-35.49
Product	Glucosamine-quanta(PEG) cation	Glucosamine-quanta(PEG)	H_2O		
	-756,821.74	-804,555.64	-47,932.31	-1,609,309.69	-4.06
Simulation by B3LYP/6-31G//HF-6-31G method					
Reactant	Di glucosamine-quanta(PEG)	H_3O^+			
	-1,561,247.08	-48,115.95		-1,609,363.04	0.00
Reactant complex	Di glucosamine-quanta(PEG)--H_3O^+				
	-1,609,330.35			-1,609,330.35	32.68
Product complex	Glucosamine-quanta(PEG) cation---Glucosamine-quanta(PEG)---H_2O				
	-1,609,416.90			-1,609,416.90	-53.86
Product	Glucosamine-quanta(PEG) cation	Glucosamine-quanta(PEG)	H_2O		
	-756,821.74	-804,589.61	-47,932.95	-1,609,344.29	18.74

Appendix Table C5 The relative energy of bond breaking of Di glucosamine-penta(PEG) in acid solution

Reaction step	Molecular energy (kcal/mol)			Total energy (kcal/mol)	Relative energy (kcal/mol)
Simulation by B3LYP/6-31G//PM3 method					
Reactant	Di glucosamine-penta(PEG)	H_3O^+			
	-1,754,187.86	-48,115.95		-1,802,303.81	0.00
Reactant complex	Di glucosamine-penta(PEG)--H_3O^+				
	-1,802,270.18			-1,802,270.18	33.63
Product complex	Glucosamine-penta(PEG) cation---Glucosamine-penta(PEG)---H_2O				
	-1,802,354.02			-1,802,354.02	-50.21
Product	Glucosamine-penta(PEG) cation	Glucosamine-penta(PEG)	H_2O		
	-853,258.70	-901,049.95	-47,932.31	-1,802,240.96	62.85
Simulation by B3LYP/6-31G//HF-6-31G method					
Reactant	Di glucosamine-penta(PEG)	H_3O^+			
	-1,754,245.31	-48,115.95		-1,802,361.26	0.00
Reactant complex	Di glucosamine-penta(PEG)--H_3O^+				
	-1,802,325.96			-1,802,325.96	35.31
Product complex	Glucosamine-penta(PEG) cation---Glucosamine-penta(PEG)---H_2O				
	-1,802,375.81			-1,802,375.81	-14.54
Product	Glucosamine-penta(PEG) cation	Glucosamine-penta(PEG)	H_2O		
	-853,309.00	-901,091.80	-47,932.95	-1,802,333.74	27.52

Appendix Table C6 The relative energy of bond breaking of Di glucosamine-mono(PEG) in normal solution

Reaction step	Molecular energy (kcal/mol)		Total energy (kcal/mol)	Relative energy (kcal/mol)
Simulation by B3LYP/6-31G//AM1method				
Reactant	Di glucosamine-mono(PEG)	H_2O		
	-982,195.49	-47,932.31	-1,030,127.81	0.00
Reactant complex	Di glucosamine-mono(PEG)---H_2O			
	-1,029,670.88		-1,029,670.88	456.92
Product complex	Glucosamine-mono(PEG)---Glucosamine-mono(PEG)			
	-1,030,056.69		-1,030,056.69	71.11
Product	Glucosamine-mono(PEG)	Glucosamine-mono(PEG)		
	-515,052.53	-515,052.53	-1,030,105.06	22.75
Simulation by B3LYP/6-31G//PM3 method				
Reactant	Di glucosamine-mono(PEG)	H_2O		
	-982,250.27	-47,932.95	-1,030,183.22	0.00
Reactant complex	Di glucosamine-mono(PEG)---H_2O			
	-1,029,708.25		-1,029,708.25	474.96
Product complex	Glucosamine-mono(PEG)---Glucosamine-mono(PEG)			
	-1,030,106.37		-1,030,106.37	76.84
Product	Glucosamine-mono(PEG)	Glucosamine-mono(PEG)		
	-515,089.67	-515,089.67	-1,030,179.35	3.87

Appendix Table C7 The relative energy of bond breaking of Di glucosamine-di(ethylene glycol) in normal solution

Reaction step	Molecular energy (kcal/mol)		Total energy (kcal/mol)	Relative energy (kcal/mol)
Simulation by B3LYP/6-31G//AM1method				
Reactant	Di glucosamine-di(ethylene glycol)	H_2O		
	-1,175,193.80	-47,932.31	-1,223,126.11	0.00
Reactant complex	Di glucosamine-di(ethyleneglycol)---H_2O			
	-1,222,761.83		-1,222,761.83	364.29
Product complex	Glucosamine-di(ethylene glycol)---Glucosamine-di(ethylene glycol)			
	-1,223,029.83		-1,223,029.83	96.29
Product	Glucosamine-di(ethylene glycol)	Glucosamine-di(ethylene glycol)		
	-611,554.20	-611,554.20	-1,223,108.40	17.71
Simulation by B3LYP/6-31G//PM3 method				
Reactant	Di glucosamine-di(ethylene glycol)	H_2O		
	-1,175,248.83	-47,932.95	-1,223,181.78	0.00
Reactant complex	Di glucosamine-di(ethyleneglycol)---H_2O			
	-1,222,721.45		-1,222,721.45	460.33
Product complex	Glucosamine-di(ethylene glycol)---Glucosamine-di(ethylene glycol)			
	-1,223,117.47		-1,223,117.47	64.30
Product	Glucosamine-di(ethylene glycol)	Glucosamine-di(ethylene glycol)		
	-611,589.36	-611,589.36	-1,223,178.73	3.05

Appendix Table C8 The relative energy of bond breaking of Di glucosamine-tri(ethylene glycol) in normal solution

Reaction step	Molecular energy (kcal/mol)		Total energy (kcal/mol)	Relative energy (kcal/mol)
Simulation by B3LYP/6-31G//AM1method				
Reactant	Di glucosamine-tri(ethylene glycol)	H_2O		
	-1,368,191.82	-47,932.31	-1,416,124.13	0.00
Reactant complex	Di glucosamine-tri(ethyleneglycol)---H_2O			
	-1,415,711.25		-1,415,711.25	412.88
Product complex	Glucosamine-tri(ethylene glycol)---Glucosamine-tri(ethylene glycol)			
	-1,416,028.02		-1,416,028.02	96.11
Product	Glucosamine-tri(ethylene glycol)	Glucosamine-tri(ethylene glycol)		
	-708,053.31	-708,053.31	-1,416,109.44	14.70
Simulation by B3LYP/6-31G//PM3 method				
Reactant	Di glucosamine-tri(ethylene glycol)	H_2O		
	-1,368,247.69	-47,932.95	-1,416,180.64	0.00
Reactant complex	Di glucosamine-tri(ethyleneglycol)---H_2O			
	-1,415,715.66		-1,415,715.66	464.98
Product complex	Glucosamine-tri(ethylene glycol)---Glucosamine-tri(ethylene glycol)			
	-1,416,105.99		-1,416,105.99	74.65
Product	Glucosamine-tri(ethylene glycol)	Glucosamine-tri(ethylene glycol)		
	-708,088.97	-708,088.97	-1,416,177.94	2.69

Appendix Table C9 The relative energy of bond breaking of Di glucosamine-quanta(ethylene glycol) in normal solution

Reaction step	Molecular energy (kcal/mol)		Total energy (kcal/mol)	Relative energy (kcal/mol)
Simulation by B3LYP/6-31G//AM1method				
Reactant	Di glucosamine-quanta(ethylene glycol)	H_2O		
	-1,561,189.67	-47,932.31	-1,609,121.98	0.00
Reactant complex	Di glucosamine-quanta(ethyleneglycol)---H_2O			
	-1,608,712.44		-1,608,712.44	409.54
Product complex	Glucosamine-quanta(ethylene glycol)---Glucosamine-quanta(ethylene glycol)			
	-1,609,026.59		-1,609,026.59	95.39
Product	Glucosamine-quanta(ethylene glycol)	Glucosamine-quanta(ethylene glycol)		
	-804,555.64	-804,555.64	-1,609,111.28	10.71
Simulation by B3LYP/6-31G//PM3 method				
Reactant	Di glucosamine-quanta(ethylene glycol)	H_2O		
	-1,561,247.08	-47,932.95	-1,609,180.03	0.00
Reactant complex	Di glucosamine-quanta(ethyleneglycol)---H_2O			
	-1,608,728.38		-1,608,728.38	451.65
Product complex	Glucosamine-quanta(ethylene glycol)---Glucosamine-quanta(ethylene glycol)			
	-1,609,120.55		-1,609,120.55	59.48
Product	Glucosamine-quanta(ethylene glycol)	Glucosamine-quanta(ethylene glycol)		
	-804,589.61	-804,589.61	-1,609,179.22	0.81

CURRICULUM VITAE

NAME : Miss Jirapat Boonmee

BIRTH DATE : October 2nd, 1984

BIRTH PLACE : Suphanburi, Thailand

EDUCATION :

YEAR	INSTITUTION	DEGREE/DIPLOMA
2002	U-Thong School	High School
2006	Kasetsart University	B.Sc. (Biochemistry; 2nd Class Honor)

SCHOLARSHIP : ADB Scholarship 2007-2009